Sequential deposition and remodeling of cell wall polymers during tomato pollen development

Syeda Roop Fatima Jaffri, Cora A. MacAlister*

Department of Molecular, Cellular and Developmental Biology, University of Michigan, Ann Arbor, MI, USA, 48109

* Corresponding author macalist@umich.edu

Key Words: pollen, exine development, intine, cell wall, tomato, anther, pectin, cellulose, callose

Length: 10,358 words, 8 figures

Abstract:

The cell wall of a mature pollen grain is a highly specialized, multilayered structure. The outer, sporopollenin-based exine provides protection and support to the pollen grain while the inner intine, composed primarily of cellulose, is important for pollen germination. The formation of the mature pollen grain wall takes place within the anther with contributions of cell wall material from both the developing pollen grain as well as the surrounding cells of the tapetum. The process of wall development is complex; multiple cell wall polymers are deposited, some transiently, in a controlled sequence of events. Tomato (*Solanum lycopersicum*) is an important agricultural crop which requires successful fertilization for fruit production as do many other members of the Solanaceae family. Despite the importance of pollen development for tomato, little is known about the detailed pollen gain wall developmental process. Here we describe the structure of the tomato pollen wall and establish a developmental timeline of its formation. Mature tomato pollen is released from the anther in a dehydrated state and is tricolpate, with three long apertures without overlaying exine from which the pollen tube may emerge. Using histology and immunostaining we determined the order in which key cell wall polymers were deposited with respect to overall pollen and anther development. Pollen development began in young flower buds when the pre-meiotic microspore mother cells (MMCs) began losing their cellulose primary cell wall. Following meiosis, the still conjoined microspores progressed to the tetrad stage characterized by a temporary, thick callose wall. Breakdown of the callose wall released the individual early microspores. Exine deposition began with the secretion of the sporopollenin foot-layer. At the late microspore stage, exine deposition was completed and the tapetum degenerated. The pollen underwent mitosis to produce bicellular pollen at which point intine formation began, continuing through to pollen maturation. The entire cell wall development process was also punctuated by dynamic changes in pectin composition, particularly changes in methyl-esterified and de-methyl-esterified homogalacturonan.

Introduction

The production of pollen was a major innovation during the evolution of land plants. The pollen grain is a highly specialized structure which includes a complex and unique cell wall supporting its functions. The mature pollen wall can be broadly divided into two layers, an outer sporopollenin-rich exine and an inner intine which has a composition similar to other plant cell walls. In addition to the differences in their composition, these two layers have markedly different developmental origins and functions (Heslop-Harrison, 1968). The exine protects the pollen cytoplasm from excess dehydration and other environmental insults and mediates adhesion to pollinators and the stigmatic surface (Zinkl et al., 1999). Once the relevant interactions between pollen and stigma take place, the pollen grain hydrates and the intine serves as the organizing site for formation of a pollen tube. Once initiated, the pollen tube expands at its tip to complete pollen germination. The pollen tube will then carry the sperm nuclei from the pollen grain through the female floral tissue to a receptive ovule (Taylor & Hepler, 1997).

Pollen development takes place in the anthers, beginning in early immature buds with the specification of microspore mother cells (MMCs) and proceeding through meiosis, microspore mitosis and pollen development to mature pollen release at anther dehiscence (Canales et al., 2002; Gómez et al., 2015; Scott et al., 2004). During this process, the cell wall is radically altered with many cell wall polymers deposited, removed, or remodeled. The mature pollen cell wall contains material produced by both the developing pollen itself and by the sporophytic tapetum, a layer of cells lining the locule cavity in which the microspores develop (Owen & Makaroff, 1995).

Before the initiation of meiosis the MMCs are surrounded by a simple primary cell wall; during early prophase the middle lamella expands followed by a reduction in the flanking fibrillous wall layers and the initiation of callose (β-1,3-glucan) deposition between the plasma membrane and the primary wall (Polowick & Sawhney, 1992). The deposition of callose continues during and after meiosis eventually producing a thick callose wall which holds the four products of meiosis in a tetrad (Owen & Makaroff, 1995; Polowick, P L; Sawhney, V, 1993a). The callose wall serves as a scaffold for exine development, first by the deposition of primexine, a poorly defined microfibrillar polysaccharide matrix formed by the microspore (Hess & Frosch, 1994). Secretion of callase by the tapetal tissue causes break down of the callose wall separating the individual microspores (Chasan, 1992; Polowick; Sawhney, 1993b; Quilichini et al., 2014; Rhee et al., 2003). The primexine serves as a scaffold for the deposition of sporopollenin produced by the tapetum. The sporopollenin polymerizes onto the primexine producing the foot layer (Quilichini et al., 2014). The exine may be further elaborated with additional sporopollenin deposition e.g., production of inner column shaped baculae, and the surface decoration tectum. Together the sporopollenin foot layer (nexine), tectum and baculae (sexine) form the mature pollen exine (Chebli et al., 2012; Jiang et al., 2013; Polowick & Sawhney, 1992; Renzaglia et al., 2020). After exine deposition, the tapetal cell layer breaks down releasing material for the outermost layer of the pollen, the pollen coat also

called pollenkitt or tryphine (El-Ghazaly & Jensen, 1986). The pollen coat is required for the pollen-stigma interface and promotes pollen hydration (Ishiguro et al., 2010), and is largely composed of proteins and lipids (Bashir et al., 2013; Piffanelli & Murphy, 1998; Rejón et al., 2016).

Concurrent with the later stages of exine formation, the intine develops. Unlike the exine which is composed primarily of specialized sporopollenin, the intine's composition is similar to that of other plant cell types with major components including cellulose, pectin and cell wall-associated proteins (Fang et al., 2008; Hess, 1993; Persson et al., 2007; Suárez-Cervera et al., 2002). The apertures, which will serve as possible sites for pollen tube initiation and pollen germination, develop an unique pollen wall, completely or partially lacking exine and, in some species, highly elaborating the intine into a specialized structure called the Zwischenkörper (Dobritsa & Reeder, 2017; El-Ghazaly et al., 1986; Picken, 1984b)

Mutants with defects in pollen wall formation have been identified in several species, providing insight into the molecular basis of pollen wall development and the roles of cell wall components. The process of exine deposition is relatively well studied, and there are many well characterized exine mutants with male sterility phenotypes (Blackmore et al., 2007; Dobritsa et al., 2011; Jiang et al., 2013; Shi et al., 2015). Broadly speaking, these mutants can be classified into overlapping functional categories including biosynthesis and transport of sporopollenin precursors, primexine formation and tryphine synthesis. Proteins falling in the sporopollenin biosynthesis class include ACYL-CoA SYNTHETASE5 (ACOS5), the fatty acyl reducatase MALE STERILE2 (MS2) along with its rice ortholog DEFECTIVE POLLEN WALL (DPW), and acyl-CoA-binding proteins (AtACBP4, 5 and 6), among others (Aarts et al., 1997; Hsiao et al., 2015; Shi et al., 2011; Souza et al., 2009; Zhang et al., 2011). Since the synthesis of sporopollenin precursors takes place in the tapetum, they must be transported into the anther locule which requires the ATP-binding cassette transporter superfamily member ABCG26/WBC27 (Choi et al., 2011; Quilichini et al., 2010). Notable primexine genes, include Arabidopsis *DEFECTIVE IN EXINE FORMATION 1* (*DEX1*) and its rice ortholog *OsDEX1* (Yu et al., 2016). DEX1 is a membrane calcium binding protein, and *dex1* pollen have reduced primexine and abnormal exine (Paxson-sowders et al., 2001). Examples of tryphine synthesis mutants include mutants of phosphoserine phosphatase, an enzyme required to catalyze the last step of phosphorylated pathway of serine biosynthesis (PPSB). These mutants show a normal exine without any tryphine (Flores-Tornero et al., 2015).

Cellulose synthesis and callose synthesis and degradation are also required for pollen wall development. Arabidopsis triple mutants in the cellulose synthase complex members *cesa6, cesa9* and *cesa2* produced deformed pollen with abnormally thickened intines, possibly due to a compensation by other cell wall polymers in the absence of cellulose (Persson et al., 2007). In Arabidopsis, the callose synthase CalS5 is required for callose wall formation and pollen fertility. In *cals5* mutants the exine wall organization is also disrupted with malformed baculae and tectum as well as randomly deposited globular tryphine, showing

that the callose wall is required for exine sculpting (Dong et al., 2005). Similarly knockdown or knockout of rice Glucan Synthase-Like 5 (GSL5) reduces callose production during pollen development, compromising exine deposition and pollen fertility (Shi et al., 2015). The timely degradation of callose is also required for pollen fertility. Rice plants silenced for the β-1,3-glucanase gene *Osg1* have delayed release of the microspores from the tetrad, leading to their degeneration and male sterility (Wan et al., 2011).

Several mutants also suggest an important roles for pectin throughout pollen development (Cankar et al., 2014; Chebli et al., 2012; Jiang et al., 2013; Phan et al., 2011; Suárez-Cervera et al., 2002). The major form of pectin, homogalacturonan (HG, β-1,4-galacturonic acid), is initially synthesized in the Golgi in a methyl-esterified form (meHG). After secretion the methyl groups may be enzymatically removed by pectin methyl-esterases (PMEs) to form de-methyl-esterified HG (dmeHG), exposing negative charges which can form Ca^{2+} salt bridges between neighboring polymers, rigidifying the wall (Bosch & Hepler, 2005). De-methyl-esterification can also promote pectin degradation by polygalacturonases (PGs) (Verlag et al., 2003). The separation of the microspores at the tetrad stage requires pectin remodeling as evidenced by the Arabidopsis *quartet* mutants (*qrt1*, *qrt2* and *qrt3*) in which the pollen completes development as a tetrad (Preuss et al., 1993; Rhee et al., 2003). *QRT1* encodes a PME and *QRT2* and *QRT3* encode PGs (Francis et al., 2006; Ogawa et al., 2009; Rhee et al., 2003; Aouali et al., 2001). Pectin remodeling is also important for the formation of the intine as demonstrated by Arabidopsis *pme48* mutants in which the intine accumulates high levels of meHG resulting in defective pollen imbibition and germination defects (Leroux et al., 2015). In Chinese cabbage, co-inhibition of two closely related PGs, Brassica campestris Male Fertility 26a (BcMF26a) and BcMF26b have defective pollen intine and severely inhibited male fertility (Lyu et al., 2015).

While broad landmarks of anther and pollen development are well known and generally conserved, the molecular events of PG wall formation have received much more limited attention, particularly with respect to the development of the intine (Gómez et al., 2015; Ma et al., 2021). Here, we focus on elucidating this process during tomato pollen development. Tomato is an important agricultural crop which requires successful pollination for fruit set (Picken, 1984). It is also highly sensitive to environmental disruptions of fertility, particularly high temperature stress (Giorno et al., 2010, 2013; Müller et al., 2016; Pressman et al., 2002) Therefore, understanding the development of pollen is an important preliminary step to safeguarding production against environmental insults. Tomato also serves as a model system for the large Solanaceae family which includes many other agriculturally important plants. Given the importance of the pollen grain wall to pollen fertility, we have established a timeline of polymer deposition and remodeling during tomato pollen grain wall formation.

Materials and Methods

Plant material and growth conditions

Solanum lycopersicum cv Micro-Tom (Carvalho et al., 2011) were grown under 16-hour light: 8-hour dark cycles in temperature-controlled growth chambers maintained at 23°C. Buds were staged by measuring the length from the bud tip to the pedicle with a vernier caliper. For scanning electron microscopy (SEM) of pollinated pistils, anthers were removed from 6mm flower buds, and pistils were covered with open 0.2ml PCR tubes and allowed to mature for 48 hours. Pollen was collected by vortexing freshly collected mature anthers in 1.5ml epitubes and applied to pistils with a paint brush. Pollinated plants were returned to the growth chamber, watered, and covered with a clear plastic dome to increase humidity. Five hours after pollination, pistils were fixed and treated for SEM as described below.

Scanning Electron Microscopy

For scanning electron microscopy (SEM), manually pollinated pistils were collected and submerged in fresh fixative (acetic acid/ethanol, 1:3), and fixed under vacuum for 2 hours. Pistils were then transferred to fresh 100% ethanol and kept at 4°C overnight in a tightly closed glass vial. The tissue was then dehydrated using chemical drying with graded hexamethyldisilazane (HDMS) (Sigma-Aldrich catalogue number 440191) series (Lee & Chow, 2012). Ethanol was slowly replaced with HDMS for 20 minutes each in an ethanol: HDMS series of 1:0, 3:1, 3:2. 1:1, 1:3, and three times 100% HDMS. Afterwards, tissue was left overnight in the HDMS in an open tube under the fume hood. In the morning, the HDMS had evaporated, and the tissue was dry and ready for gold coating. Tissue was attached to SEM stubs with double sided tape, and sputter coated with gold particles in vacuum at 200mAmps for 120 seconds (~15-20nm of gold) using a Denton Desk II sputter coater. For imaging of pollen grains, dry mature pollen grains were collected in epitubes from healthy, mature dehiscent flowers. Pollen was sprinkled on adhesive SEM stubs with paint brush bristles and sputter coated with gold particles in vacuum for 90 seconds. Gold coated pollen and pistils were imaged using EMAL JEOL JSM-7800FLV field-emission scanning electron microscope. For pore diameter measurements, three random pictures each of four individual pollen grain were taken, and diameters of all the pores in each micrograph were measured. The shown values are average across all measurements.

Transmission electron microscopy

Pollen grains were suspended in ice cold fixative containing 2% formaldehyde, 2.5% glutaraldehyde, 0.025M PIPES buffer pH 7.2, and 0.001% tween20 via vortexing. After two hours incubation under vacuum, the solution was replaced with fresh fixative and vials were sealed and kept at 4°C overnight. Pollen was then pelleted by centrifugation at room temperature and washed with 0.025M phosphate buffer pH 7 for ten minutes, followed by a PIPES buffer pH 7.2 wash for twenty minutes. Pollen was then post fixed in 1% osmium tetroxide (Sigma-Aldrich catalogue number 75633) in phosphate buffer pH 7 for one hour. This was followed by another ten-minute phosphate buffer wash followed by twenty minutes

PIPES buffer wash. Pollen was then dehydrated for twenty minutes each in an ethanol series (25%, 35%, 50%, 70%, 80%, 90%, and three times 100%). Ethanol was then replaced slowly with LR white plastic polymer (Agar Scientific catalogue number AGR1281), by an LR white: ethanol series of 1:3, 2:3, 1:1, 3:2, 3:1,1:0, 1:0, 1:0 with each step of the series having a 4°C incubation of twenty-four hours. At this stage pollen was put in a gelatin capsule with fresh LR white and polymerized at 58°C for twenty-four hours. Solid polymer blocks were sectioned into 80nm ultrathin sections and stained with 7% uranyl acetate and lead citrate. Sections were imaged with JOEL JEM-1400 plus electron microscope with a XR401 SCMOS camera. For cell wall measurements, three pollen grains were measured at ten random positions per grain, excluding the apertures, the average across all measurements was taken.

Paraffin embedding, sectioning and toluidine blue staining.

To identify appropriate bud length for each pollen development stage, flower buds of 2mm, 4mm, 5mm, 6mm, 8mm and fully mature dehiscent flowers were fixed by submerging in ice cold fixative (4% PFA and 0.3% Tween20 in PBS) and vacuum infiltrated for 20 minutes. Fresh fixative and vacuum were applied until the tissue sunk to the bottom. The tissue was then dehydrated in a PBS-ethanol series of 10%, 30%, 50%, 70%,85% and 100% ethanol for 1 hour each at 4°C. The tissue was then infiltrated with histoclear (Avantor, Electron Microscopy sciences, catalog number 101412-878) in an ethanol: histoclear series (3:1, 1:1, 0:1, 0:1, 0:1) at room temperature. Histoclear was then slowly replaced with molten paraffin at 60°C, by replacing the histoclear with a histoclear: paraffin series (3:1, 1:1, 1:3, 0:1, 0:1, 0:1) for 24 each at 60°C. Final paraffin embedded tissue was sectioned with a microtome to 8µm thick sections and placed on poly-lysine coated slides. Sections were dewaxed by submerging in histoclear and dehydrated by dipping in an ethanol series (10%, 30%, 50%, 70%, 85% and 100%) ethanol in PBS. Dewaxed and dehydrated sections were stained with 0.1% toluidine blue (Cankar et al., 2014) by applying the stain and heating the slide to 60C for 30 seconds. After stain application, slides were washed with distilled water and permanently mounted by applying Permount (Fischer Scientific catalog number SP15-500) and cover slip.

LR white embedding, semi-thin sectioning, and immunostaining

Immunohistochemistry analysis was done as previously described (Luis da Costa et al., 2017). Briefly, flower buds of the appropriate length were removed from the plant, and for buds bigger than 2mm the anthers were dissected out. The tissue was fixed and LR white embedded as described for TEM above, without the osmium tetroxide post-fixation step. Hardened samples were sectioned with glass knife ultra-microtome in 200nm semi-thin sections. Sections were observed and imaged with light microscopy by staining with 0.1% toluidine blue in water. For calcofluor white staining, one drop of calcofluor white solution (containing Calcofluor White1g/l, Evans blue 0.5g/l; Sigma-Aldrich, 18909) was added to the well of the slide and imaged after applying the coverslip. For aniline blue staining of callose, one drop of aniline blue fluorochrome (0.1mg/mL in distilled water; Biosupplies,18909) was applied to the well of the

slide and imaged after applying the coverslip. For immunostaining, sections were place in welled 0.001% poly-L-Lysine coated slides. After drying at 50C overnight, sections were incubated in blocking solution (5% nonfat dried milk in 1x PBS) for ten minutes in a humid chamber. Then the sections were washed for 10 minutes with PBS. Sections were incubated at room temperature for two hours followed by 4°C incubation overnight in primary antibody solution (Rat monoclonal LM19 or LM20; 1:5 antibody in blocking solution; Verhertbruggen et al., 2009). Sections were then washed twice with PBS for ten minutes and then incubated with secondary antibody solution (Anti-Rat conjugated with FITC, Sigma-Aldrich, F6258; 1:100 in blocking solution) for 3-4 hours at room temperature in the dark. Sections were then washed twice with PBS for ten10 minutes each. Sections were imaged after adding one drop of calcofluor white and applying a drop of Vectashield® antifade (Vector laboratories catalog number H-1000-10) and applying the coverslip. Sections were imaged using Leica SP5 laser scanning confocal microscope.

Results

The structure of mature tomato pollen

To observe the general shape and structure of the tomato pollen, we imaged mature released pollen grains using scanning electron microscopy (SEM). SEM micrographs showed that the tomato pollen exhibit features of a typical dicot pollen grain, with a prolate spheroid shape containing three radially equidistant elongated apertures (Figure 1A). The outer surface of the pollen was textured with spines of exine interspersed with small pores with an average diameter of 38±9nm (Supplemental Figure1 B, C and D).

To observe the internal morphology of the pollen grain, we used transmission electron microscopy (TEM) to image transverse sections of the mature pollen grain (Figure 1B). Inside, the pollen was populated with an extensive ER network, vegetative and generative nuclei, numerous mitochondria, vacuoles as well as starch granules. In some sections golgi stacks were also visible. Upon close-up examination of the pollen wall structure (Figure 1C), intine was apparent as the inner, lighter, less electron dense layer around the pollen compared to the outer exine which stained much darker. The layered organization of the exine was also apparent with the nexine layer directly adjacent to the intine, followed by the columnal baculae and finally the outermost tectum layer (Figure 1C). We measured the thickness of the overall pollen wall (658.54±58 nm) and the cell wall layers (intine 151±28nm, sexine 398±38nm, nexine 112±30nm). The intine wall was continuous around the perimeter of the pollen grain, but exine was absent at the apertures. At the apertures, while the exine was absent, the inner layer of intine formed a curved outward projection at the aperture site, called the Zwischenkörper. The intine at this site was thickened and with a layered and spongy appearance (Figure 1D).

Pollen development stage correlates with flower bud length.

To establish a reproducible staging method for pollen development we compared the morphology of anthers and developing pollen in toluidine blue stained sections of floral buds at various bud sizes. We

found that flower bud length correlated well with developmental stages of the pollen grain and could be effectively used to non-destructively estimate the developmental stage of the pollen (Figure 2A).

In the anthers of 2mm long buds, the microspore mother cells (MMCs) were visible with enlarged nuclei (Figure 2B, C and D). Cells in the center of the anther were continuous at this stage without locular pockets (Figure 2B, Supplemental Figure 2A). At the 4mm bud stage, meiosis was complete, and the meiotic products were still joined in a tetrad. The tetrad cells had distinct centrally located nuclei with no obvious vacuoles or visible nucleolus. The thick pollen wall did not stain with toluidine blue at this stage, but its outer edge was visible in sections (Figure 2B, C and D). In the anther, there was a distinct tapetal cell layer surrounding four locular pockets, a larger and a smaller pocket in each anther lobe (Supplemental Figure 2B).

Pollen in the 5mm flower buds were at the early microspore stage. The microspores had an ameboid shape and their nuclei had a distinct outline and visible nucleolus (Figure 2B, C and D). In the anthers, the locules on each side of the anther had considerably enlarged but were still separated by interlocular septa and were still lined with a distinct visible tapetum cell layer (Supplemental Figure 2C). By this stage, the non-staining tetrad wall had disappeared. In the 6mm flower bud the first pollen mitosis had occurred, producing bicellular pollen with a more rounded shape and a large central vacuole. The anthers were yellow and the two locule pockets on each side had joined to make one continuous locule cavity after the deterioration of interlocular septa (Supplemental Figure 2D). The tapetum had also broken down, with the leftover vestiges visible in the locular cavity and around the pollen.

Pollen in the 8mm flower was fully mature with a well-rounded shape and one or two nuclei visible in sections. In tomato, the second pollen mitosis, producing the two sperm nuclei occurs during pollen tube elongation (Brukhin et al., 2003). The pollen at this stage also had a distinct, two layered wall differentially stained with toluidine blue. The purple inner layer was especially prominent at the aperture sites. The pollen also contained abundant, unstained starch granules (Figure 2B, C and D). The tapetum had fully disappeared. The flower was open, and the anther was close to dehiscence upon breakage of the weak anther stomium (Figure 2A).

Exine deposition occurs post tetrad.

Sporopollenin is a distinct biological polymer, composed of fatty acid derivatives and phenolic compounds (Blackmore et al., 2007; Piffanelli et al., 1998). It is only found in the exine layer of the pollen grains and plant spores and is one of the most resilient biological molecules. Toluidine blue (TD) is a basic thiazine metachromatic dye and differentially stains acidic residues with high affinity (Sridharan & Shankar, 2012). Since sporopollenin is acidic it stains differently with toluidine blue stain (bluer as compared to intine which stains purple) (Dobritsa et al., 2011). We used toluidine blue stained sections to observe exine

deposition in developing pollen. After no cell wall staining with TD in the tetrad stage (4mm buds), a thin layer of exine was visible in the early microspores (5mm bud) (Figure 3A). This foot layer had visible breaks at the slightly invaginated future aperture sites (Figure 3A, right). In the bicellular pollen stage (6mm bud), the exine was much thicker, indicated by a thicker, bluer pollen outline and the aperture sites were visible as indentations in the exine (Figure 3B). By this stage tapetum had degenerated, leaving behind pollenkitt and pollen coat particles. In the 8mm buds, the mature pollen had a solid blue outline, showing a fully developed exine wall, as well as a differentially stained intine also clearly visible (Figure 3C).

Cellulose and callose dynamics

While certain cell wall changes were apparent in sections stained with toluidine blue, the status of other cell wall polymers required further investigation. Therefore, to follow pollen wall development, we stained anther sections of the defined developmental stages with various carbohydrate-binding dyes and cell wall antibodies. The fluorescent dye Calcofluor white is a fluorochrome with a high affinity for cellulose (β-1,4-glucan) and chitin and is regularly used to observe pollen intine, though it also possesses some affinity for callose (Fang et al., 2008; Herburger & Holzinger, 2016; Li et al., 2017; Renzaglia et al., 2020; Takebe et al., 2020). Aniline blue fluorochrome (ABF) is a callose-specific dye often used to stain pollen tube cell walls (Fang et al., 2008; Herburger & Holzinger, 2016; Renzaglia et al., 2020).

In 2mm buds, calcofluor white weakly stained the MMC cell walls, but strongly stained the cell walls of the surrounding anther tissue, suggesting reduced cellulose content in the MMC walls (Figure 4A). In 4mm buds, the tetrad-stage pollen wall stained strongly with both calcofluor white (Figure 4B) and ABF (Figure 5). ABF did not stain the pollen or the surrounding anther tissue during any other stage of development (not shown). After dissolution of the transient callose wall, in 5mm buds no calcofluor white signal was observed around the uninucleate microspore (Figure 4C), although light microscopy at this stage had shown there is a thin wall around the pollen (Figure 2D). In the 6mm bud, the bicellular pollen had a thin rim of calcofluor white signal, but robust signal at the aperture sites, consistent with the development of the thick intine of the Zwischenkörper (Figure 4D). In the mature pollen in the 8mm flower bud the pollen had a continuous calcofluor white-positive layer around the perimeter of the pollen with particularly prominent signal at the apertures (Figure 4E).

Pectin dynamics

To examine the pattern of meHG and dmeHG during pollen development, we immuno-stained anther sections with rat monoclonal antibodies LM20 and LM19 (Verhertbruggen et al., 2009). LM19 preferentially binds HG with a lower degree of esterification (i.e. deHG), while LM20 shows a complementary affinity, binding to more heavily methylated HG, though a degree of overlap does exist in their binding abilities (Christiaens et al., 2011). As a preliminary to the use of these antibodies, we first

demonstrated that the fluorophore-conjugated secondary antibody did not bind to our anther sections (Supplemental Figure 3).

In the 2mm bud, while the MMCs had weak calcofluor signal indicating low levels of cellulose, the LM20 signal was robust and generally stronger than that of the surrounding anther tissue (Figure 6A). Close-up observation of the MMC walls showed boundaries of each cell thickly marked with LM20. To observe the pattern of dmeHG at this stage, we also stained with LM19. While the boundaries of MMCs did stain with LM19, the signal was considerably less robust than that of LM20 and generally the MMC signal was consistent with the signal observed for the cell wall of the surrounding anther cells (Figure 6B).

At the tetrad stage in the 4mm bud the callose wall also stained positive for the LM20 and LM19 epitopes, (Figure 6C and D). At this stage, the LM19 signal was more robust, and the tetrad walls were strongly stained relative to other anther cells (Figure 6D). Therefore, the pollen wall at the tetrad stage contained abundant meHG and dmeHG in addition to callose (Figure 5). However, at the early microspore stage in 5mm buds, pectin distribution was largely altered. meHG, as detected by LM20 binding, was considerably reduced with only a faint signal detectable around the microspores, though the surrounding anther tissue stained robustly (Figure 7A). The LM19 signal at this stage was similarly reduced compared to the tetrad stage, but a clear outline of the microspore was visible and was more robust than the corresponding LM20 signal (Figure 7B). Therefore, the loss of the callose wall coincided with a major loss of pectin during the transition between the tetrad and microspore stage.

In the bicellular stage pollen in the 6mm bud, we observed a diffuse LM20 signal throughout the pollen. In addition, we also found robust signal at the inner surface of the aperture sites (Figure 8A). The LM19 signal was similarly diffuse in the pollen grain but was not enriched at the aperture sites at this stage (Figure 8B). In the mature pollen in the 8mm buds, there was a distinct boundary around the pollen with LM20 signal (Figure 8C) and a similar, though more robust boundary of LM19 signal (Figure 8D). The mature apertures sites were robustly stained with calcofluor white at this stage but were generally deficient in LM19 and LM20 signal relative to the non-aperture regions of the pollen wall.

Discussion

The transition from the general cell wall of a non-specialized anther cell to the structurally distinct wall of the mature pollen grain requires considerable remodeling. Here, we have combined imaging techniques to observe the structure of the tomato pollen wall and to establish the sequence of cell wall polymer remodeling events taking place during pollen development beginning with the MMCs and continuing to pollen maturation (Figure 9). In the premeiotic anthers of 2mm buds, we observed significant differences in cell wall composition between the MMCs and the surrounding anther cells. Weak calcofluor white staining (Figure 4A) and robust LM20 signal (Figure 6A) in the cell walls of the MMCs is consistent with a reduction in cellulose and higher levels of meHG in these cells compared to other anther cells. These

observations support the interpretation of previous tomato anther TEM data which described an approximately ten fold expansion of the width of the middle lamella between premeiotic MMC and those in early prophase and the loss of microfibrils adjacent to the plasma membrane by late prophase (Polowick & Sawhney, 1992). Reduced cellulose combined with increased meHG would be consistent with a more extensible cell wall, possible facilitating the expansion and remodeling required for further pollen development. Therefore, even in this early stage of pollen development, the cell wall composition of the pollen lineage cells was already distinct.

At the tetrad stage in 4mm buds, a thick callose wall surrounding the post-meiotic tetrads was apparent in ABF-stained sections (Figure 5). Unlike cellulose which is a common plant cell wall component, callose occurs transiently during cell division and in some specialized cell types or under specific conditions (Chasan, 1992; Mollet et al., 2013; Renzaglia et al., 2020). The tetrad stage was the only stage at which we observed callose and it was limited to the tetrad wall. While the ABF signal indicating the presence of callose was clear, the observation of calcofluor white binding at this stage (Figure 4B) must be interpreted with caution as it may indicate the presence of cellulose or might result from non-specific binding to callose. In terms of pectin content, we observed both LM20 and LM19 signal, indicating that the tetrad wall also contained HG of low and high degrees of methylesterification (Figure 6B). Furthermore, enhancement of LM19 signal in the tetrad wall suggests that dmeHG might serve a significant functional role here, possibly providing stiffness to the callose wall. Lack of aniline blue staining in the 5mm bud anther demonstrated that the callose wall is temporary and after meiosis degrades to separate the tetrads into individual microspores (Kravchik et al., 2019; Owen & Makaroff, 1995; Paxson-Sowders et al., 1997; Polowick; Sawhney, 1993a; Zhang et al., 2020). At this stage, most of the LM19 and LM20 signal was also lost (Figure 7). These observations are also consistent with the effect of the Arabidopsis *qrt* mutants and their disruption of pectin remodeling enzymes blocking tetrad separation (Preuss et al., 1993; Francis et al., 2006; Ogawa et al., 2009; Rhee et al., 2003; Aouali et al., 2001). Calcofluor white signal was also weak in the early microspore stage (Figure 4C), indicating little cellulose. We also detected a thin layer of exine at this stage, which may further support the wall structure (Figure 3). The primexine has an important function during this stage, unfortunately, the composition of the primexine is poorly understood, making it difficult to study (Li et al., 2017; Wang & Dobritsa, 2018). Other possible microspore cell wall components include cell wall-associated proteins, for example the extensins or arabinogalactan glycoproteins (AGPs). The extensins are moderately glycosylated, highly-repetitive proteins which can be covalently cross-linked in the wall by secreted peroxidases, possibly forming a scaffold for pectin assembly (Cannon et al., 2008; Petersen et al., 2021; Schnabelrauch et al., 1996). In Arabidopsis *peroxidase9* (*prx9*) and *prx40* double mutants, microspores and tapetal cells have a swollen phenotype suggesting compromised cell wall integrity due to a reduction in extensin crosslinking during pollen development (Jacobowitz et al., 2019). Evidence for possible AGP involvement at this stage of pollen development comes from *UNEQUAL PATTERN OF EXINE1/KAONASHI4* (*UPEX1/KNS4*), a β-(1,3)-

galactosyltransferase responsible for the synthesis of the AG glycans found on AGPs and rhamnogalacturonan I, a pectic polysaccharide. *upex1/kns4* mutants have lower levels and an altered pattern of AGPs at the microspore stage and disrupted primexine formation and exine patterning (Dobritsa et al., 2011; Li et al., 2017; Suzuki et al., 2017).

The aperture sites began to take on a distinct cell wall identity by the bicellular stage (6mm buds) when the cytoplasmic face of the future aperture sites accumulate cellulose and meHG as indicated by LM20 signal (Figure 8A). The accumulation of LM20 at this location suggests delivery of newly synthesized meHG through targeted exocytosis to these sites. By the mature stage, the apertures had a complex organization with a calcofluor-positive inner core and a ring rich in LM19 and LM20 epitopes visible in some pollen sections (Figure 8C and D). The completion of wall development in the inter-aperture regions was marked by the return of reinforcing polymers. The return of cellulose to these regions was a relatively late event since calcofluor white signal returned when exine deposition is almost complete at the 8mm stage. The later stages of pollen development were also associated with changes in pectin content. In particular, the LM19 pollen wall signal was weak in the bicellular pollen stage, but much more robust in the mature pollen, forming a continuous layer around the pollen grain. This result suggests considerable enzymatic conversion of meHG to dmeHG between these stages. The defective intine produced by Arabidopsis *pme48* mutants, which are compromised in the reduction of meHG, suggests this conversion is important for ultimate intine formation and function during pollen hydration(Leroux et al., 2015).

Despite similarities in the overall process of pollen wall development, different species produce pollen with markedly different forms. This is particularly apparent for the structure of the exine which is easily observable and, due to the resistance of sporopollenin to degradation, highly stable in the environment. Pollen also vary in the number, shape and positioning of their apertures with some groups lacking them entirely (Furness, 2007). Apertures serve not only as the sites for pollen tube initiation, but also facilitate hydration, communication with the stigma and help accommodate volume changes required during dehydration and rehydration(Matamoro-Vidal et al., 2016). Like many dicots, including Arabidopsis, tomato pollen is tri-aperturate, with exine deposition excluded from the aperture regions (Figure 1B). Our observation of pollinated pistils using SEM showed all pollen tubes originating at the aperture site, suggesting that tomato pollen germination is constrained to the aperture sites. However, this is not the case for Arabidopsis and several other species in the Brassicaceae where pollen have been observed to germinate at inter-aperture regions, taking the shortest path to the stigma (Edlund et al., 2016). One possible explanation for this difference between obligate-aperturate (tomato) and omni-aperturate (Arabidopsis) pollen maybe differences in inter-aperture region pollen wall stiffness (Edlund et al., 2016; Furness & Rudall, 2004). However, this possible difference in mechanical properties cannot be simply due to differences in exine thickness as Arabidopsis pollen exine is thicker (~1μm) compared to that of tomato (~0.5μm) (Dobritsa et al., 2011; Li et al., 2017). In careful examination of the pollen surface, we

also noted the presence of small pores (38±9nm) which were also visible in TEM sections as exine channels (Figure 1C). While the mechanism of their development and the exact chemical nature of the lining of these channels is unknown, they are ubiquitous among land plants and it is hypothesized that they facilitate hydration in advance of pollen germination. (Edlund et al., 2004).

Because pollen wall development is a highly dynamic and complex process, understanding how the pollen wall is constructed requires a temporal understanding of the events of pollen wall remodeling. The work presented here describes the changes of the major cell wall polymers during pollen development in tomato (Figure 9) and will serve as a useful reference point for studies of the perturbation of the pollen wall in this important agricultural species.

Funding

This work was supported by the National Science Foundation under grant no. IOS-1755482.

Acknowledgements

We would like to thank Gregg Sobocinski (University of Michigan, Ann Arbor) in the Molecular, Cellular and Developmental Biology (MCDB) department, Imaging Core for training and help with ultra-microtome sectioning, and confocal microscopy. We would also like to thank Sasha Meshinchi (University of Michigan, Ann Arbor) in the Biomedical research core facilities, Microscopy Core for training and help with Transmission electron microscopy. We would also like to thank Dr. Owen K. Neill at the Robert B. Mitchell Electron Microbeam Analysis Lab, part of the University of Michigan's Department of Earth and Environmental Sciences for training and help with Scanning electron microscopy.

Figure legends

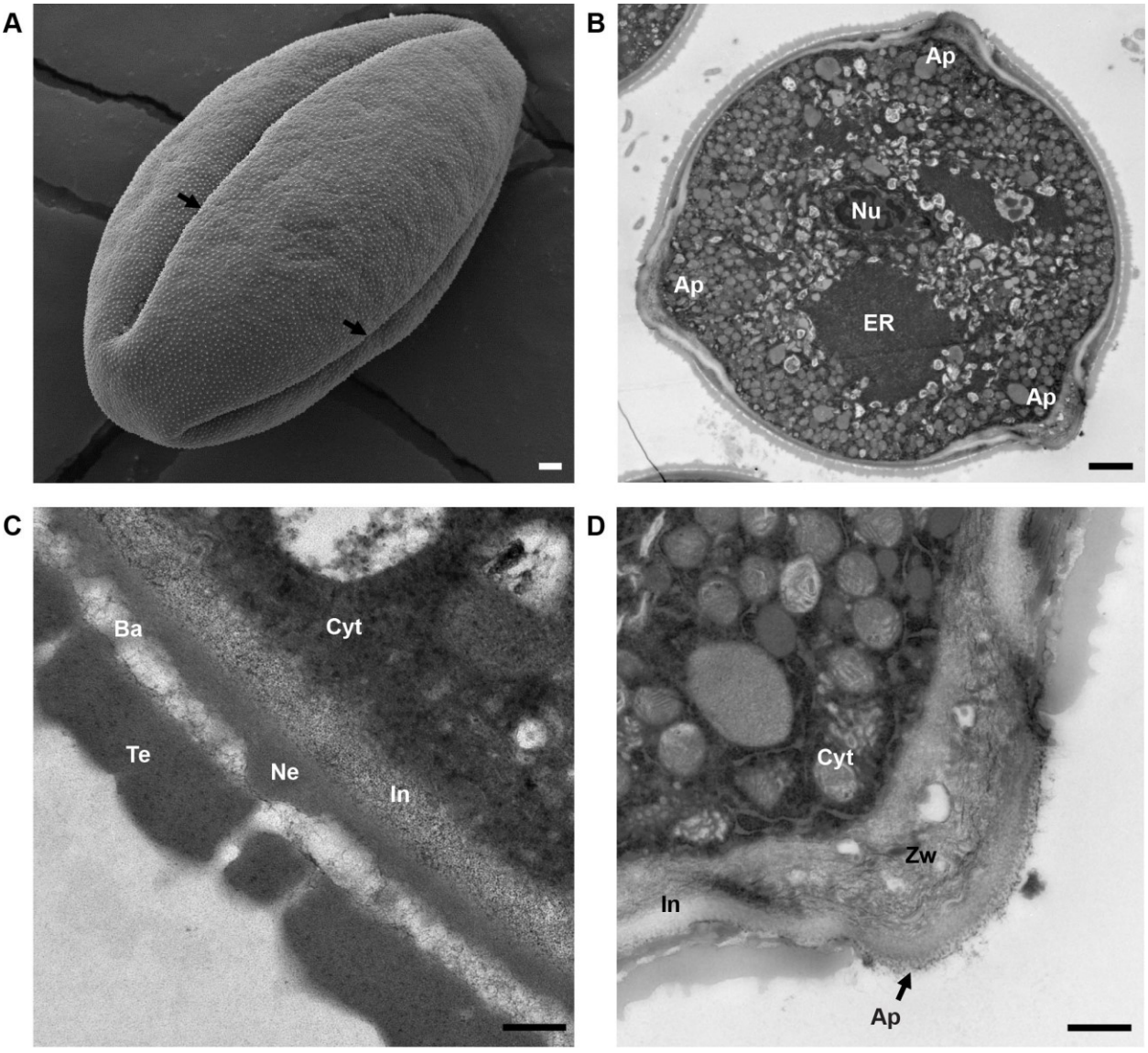

Figure 1 Structure of mature tomato pollen grain.

A. Scanning electron micrograph of a mature, released tomato pollen grain. Arrows mark the apertures (Ap). **B.** Transmission electron micrograph of a mature pollen grain cross section. Nu, nucleus; ER, endoplasmic reticulum; Ap, aperture. **C.** TEM of mature pollen showing the layers of the pollen wall. Cyt, cytoplasm; In, intine; Ne, nexine; Ba, bacula; Te, tectum. **D.** TEM close-up of pollen aperture. Arrow marks the aperture. Cyt, cytoplasm; In, intine; Zw, zwischenkorper. Scale bars 1μm in A, 2μm in B, 200nm in C and 600nm in D.

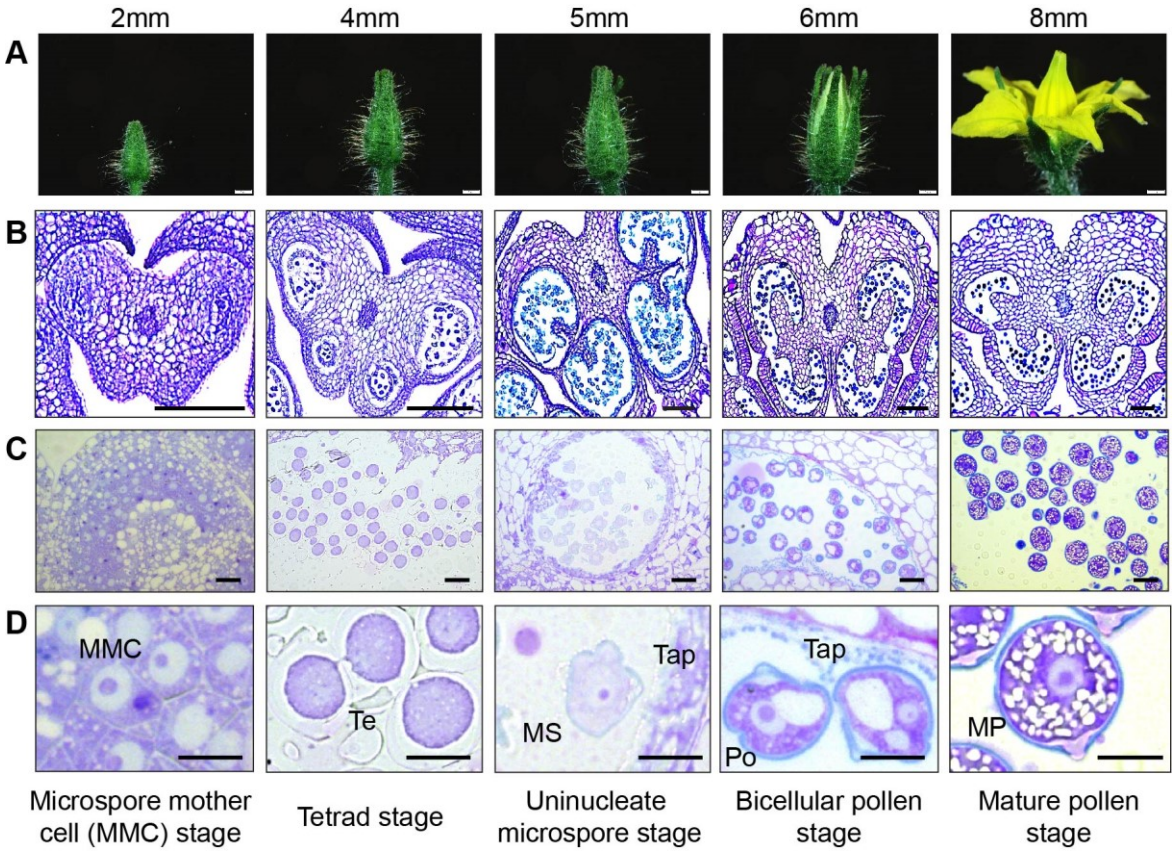

Figure 2 Tomato pollen development staging.

A. photographic series of floral development in tomato, with bud length as a marker for each stage in pollen development inside the anther. Bud lengths 2mm (microspore mother cell stage), 4mm (tetrad stage), 5mm (uninucleate microspore stage), 6mm (bicellular pollen stage) and 8mm (mature pollen stage). **B.** Micrographs of paraffin embedded 8μm thick anther cross sections stained with toluidine blue. **C.** Micrographs of LR White embedded 500nm thick anther cross sections, also stained with toluidine blue. **D.** Developing pollen grain at higher magnification, close-up of individual cells. MMC, microspore mother cell; Te, tetrad; MS, microspore; Tap, tapetum; Po, pollen; MP, mature pollen. Scale bars 1mm in A, 100μm in B, 20μm in C and 10μm in D.

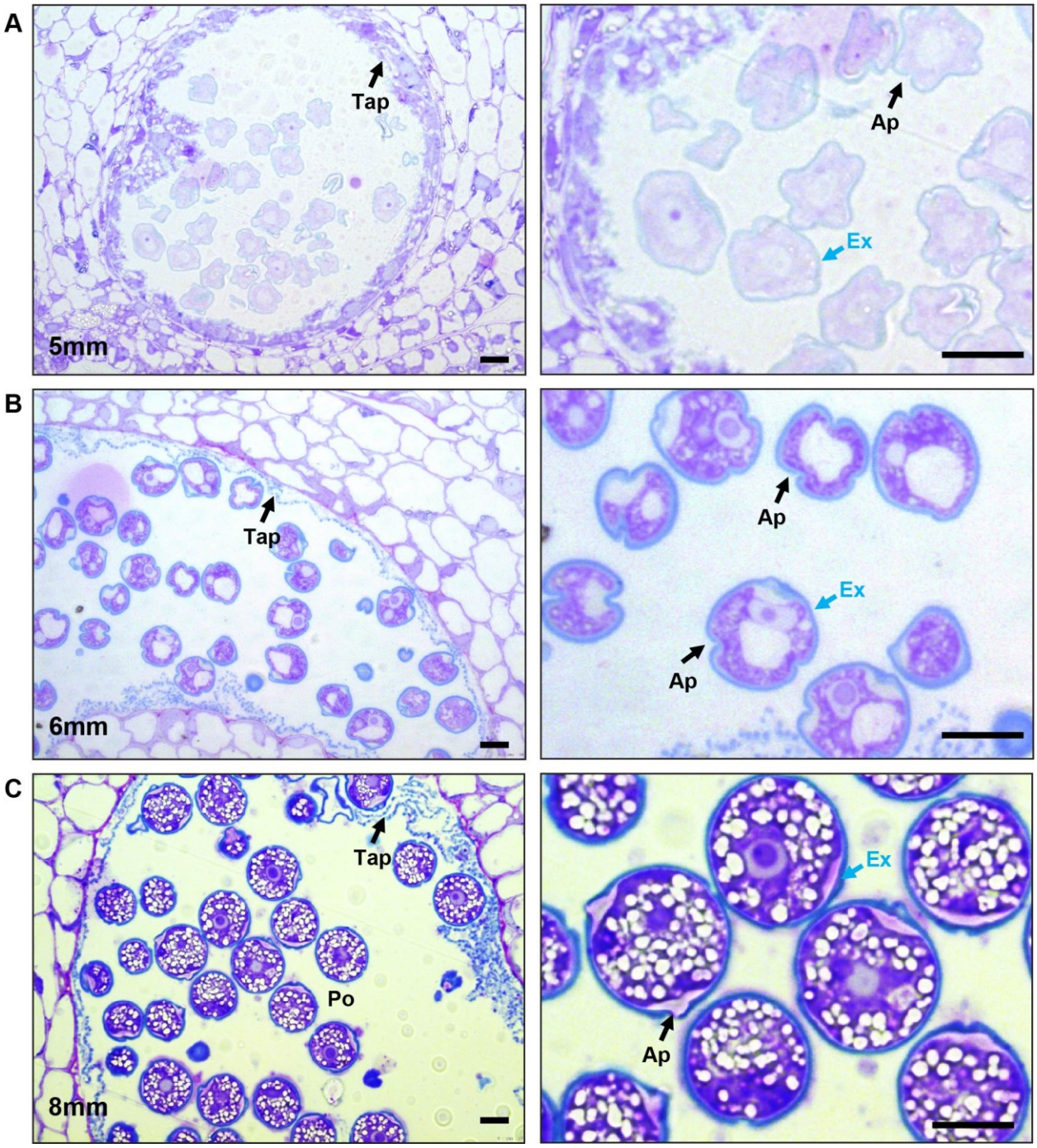

Figure 3 Progression of exine deposition.

Micrographs of LR White embedded 500nm thick anther cross sections, stained with toluidine blue **A.** Uninucleate microspore stage at 5mm bud length. Cross section of anther locule (Left), Arrow marks the tapetum. Close up of microspores (Right), Black arrow marks aperture, Blue arrow marks the exine. **B.** Bicellular pollen stage at 6mm bud length. Cross section of anther locule (Left), Arrow marks the tapetum. Close up of microspores (Right), Black arrow marks aperture, Blue arrow marks the exine. **C.** Mature pollen stage at 8mm bud length. Cross section of anther locule (Left), Arrow marks the tapetum.

Close up of microspores (Right), Black arrow marks aperture, Blue arrow marks the exine. Ex, exine; Tap, tapetum; Po, pollen; Ap, aperture. All scale bars are 10μm.

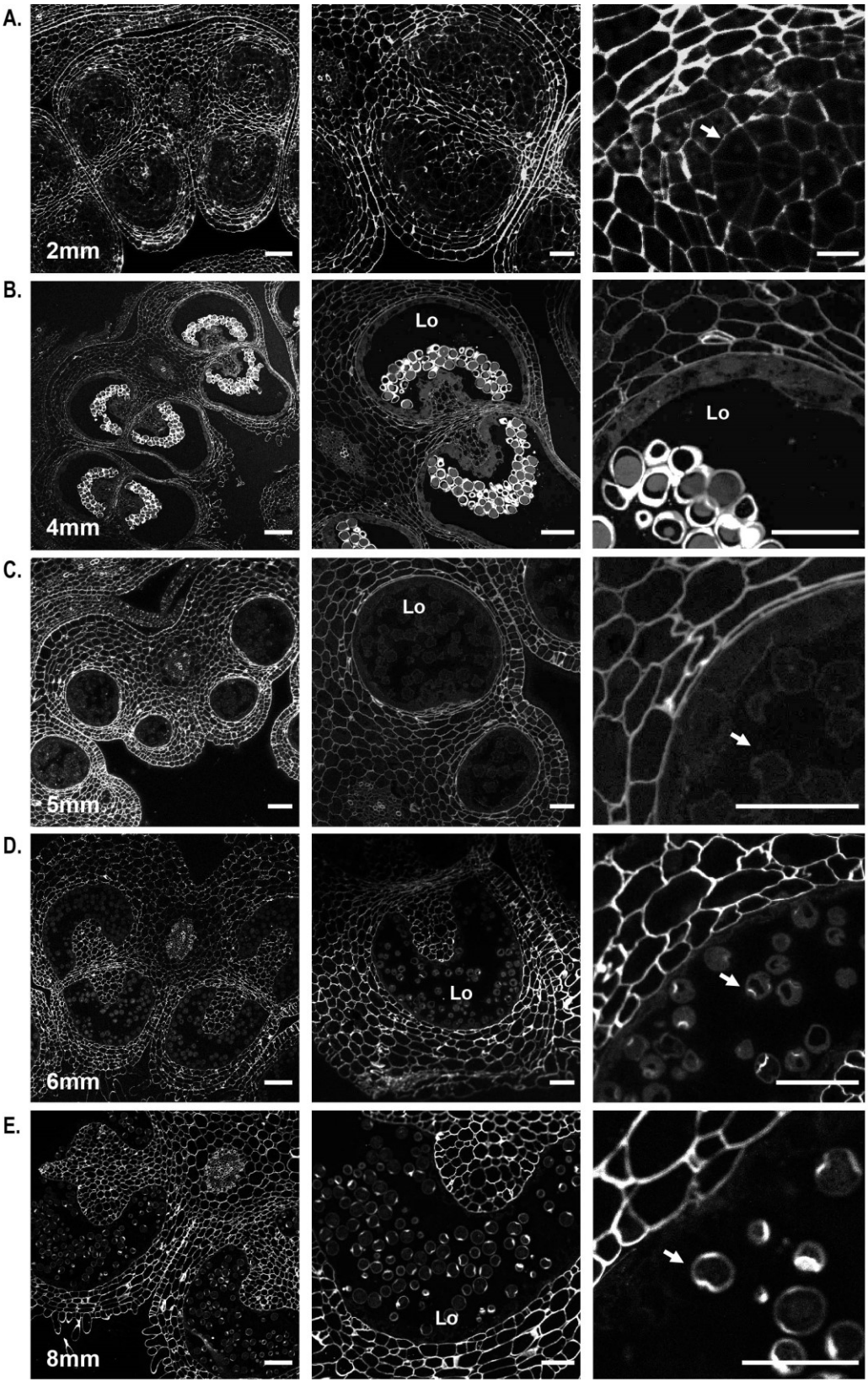

Figure 4 Calcofluor white staining of pollen development.

Fluorescent micrographs of anther cross sections (500nm) in LR white, stained with calcofluor white. **A.** Microspore mother cell stage in the 2mm bud anther. **B.** Tetrad stage in the 4mm bud anther. **C.** Uninucleate microspore stage in the 5mm bud anther. Arrow marks the microspore wall. **D.** Bicellular pollen in 6mm bud anther. Arrow marks the pollen wall. **E.** Mature pollen in 8mm bud anther. Arrow marks pollen wall. Te, tetrad. Scale bars **A.** 50μm (Left), 25μm (Center and Right). **B.** 75μm (Left) 50μm (Center and Right). **C.** 50μm (Left) 25μm (Center and Right). **D.** 75μm (Left) 50μm (Center and Right). **E.** 75μm (Left) 50μm (Center and Right).

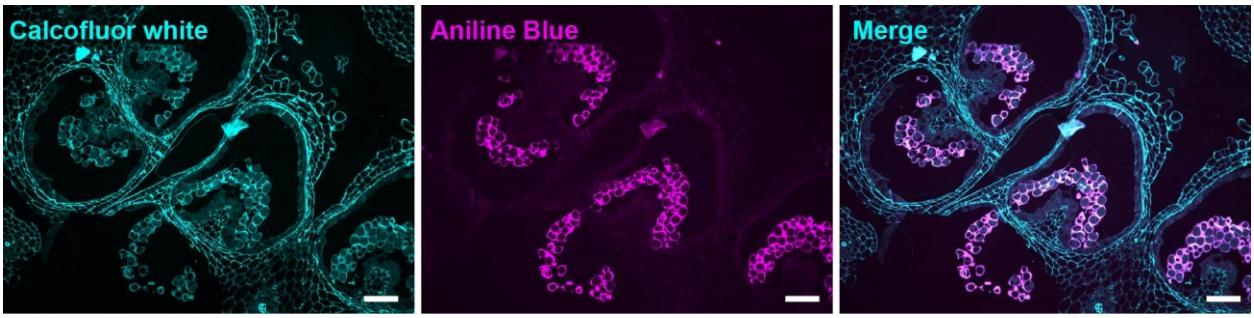

Figure 5 Aniline blue staining of the tetrad callose wall.

Fluorescent micrographs of anther cross sections (500nm) in LR white, of the 4mm bud anther, stained with calcofluor white and aniline blue fluorochrome. Calcofluor white staining (Cyan) **(Left).** Aniline blue staining (Magenta) **(Center).** Merged staining **(Right).** Scale bars 50μm.

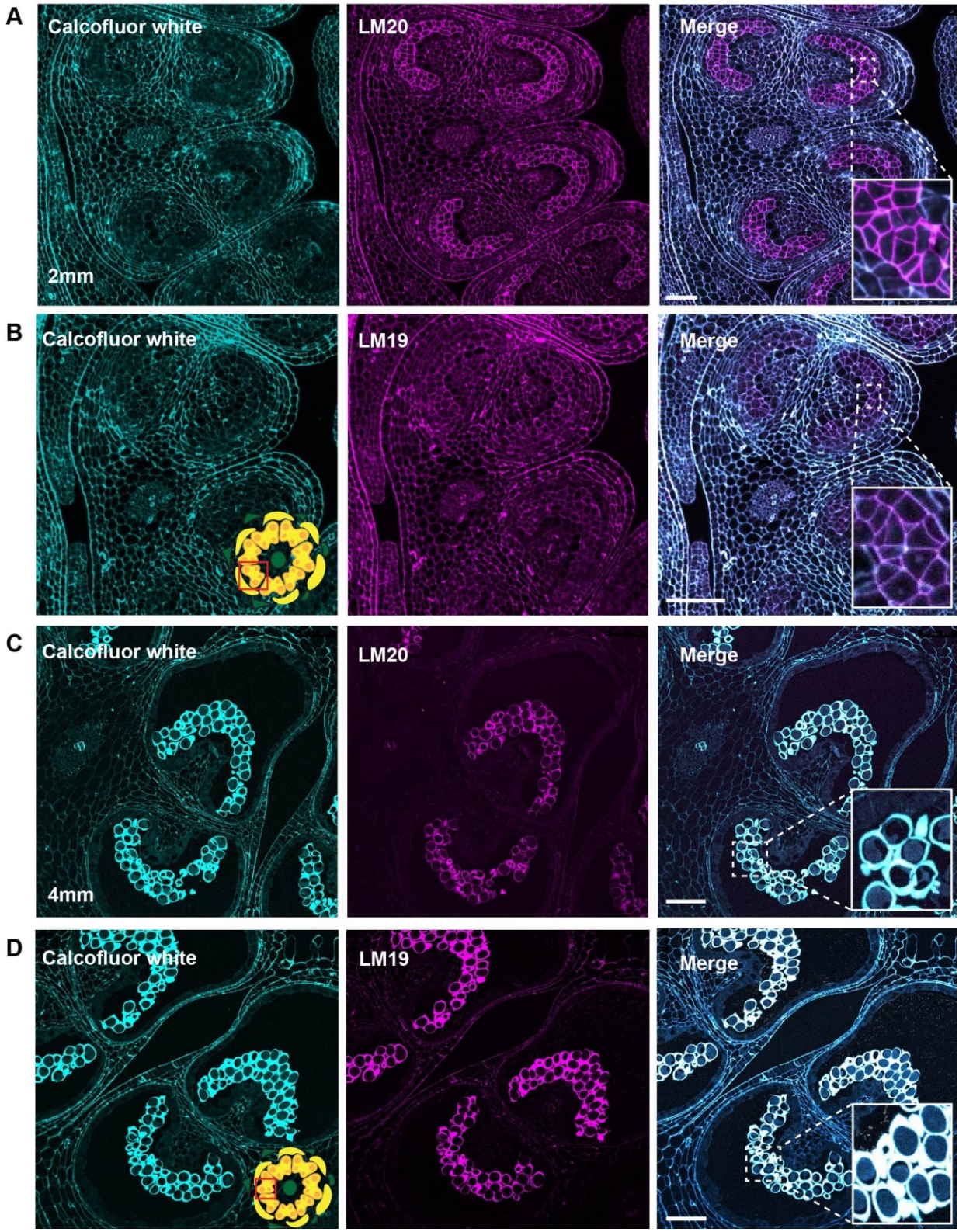

Figure 6 LM20 and LM19 immunostaining of the 2mm and 4mm bud anthers.

Fluorescent micrographs of anther cross sections (500nm) in LR white, of the 2mm and 4mm bud anther, stained with Calcofluor white and FITC conjugated anti-rat secondary for LM20 or LM19.

Calcofluor white staining (Cyan) (Left). Aniline blue staining (Magenta) (Center). Merged staining (Right). **A**. LM20 staining of the 2mm anther. Right panel inset showing zoomed in view of the MMCs wall with the merged staining. **B**. LM19 staining of the 2mm anther. Right panel inset showing zoomed in view of the MMCs with the merged staining **C**. LM20 staining of the 4mm anther. Right panel inset showing zoomed in view of the tetrad cells with the merged staining **D**. LM19 staining of the 4mm anther. Right panel inset showing zoomed in view of the tetrad cells with the merged staining. Scale bars 50µm.

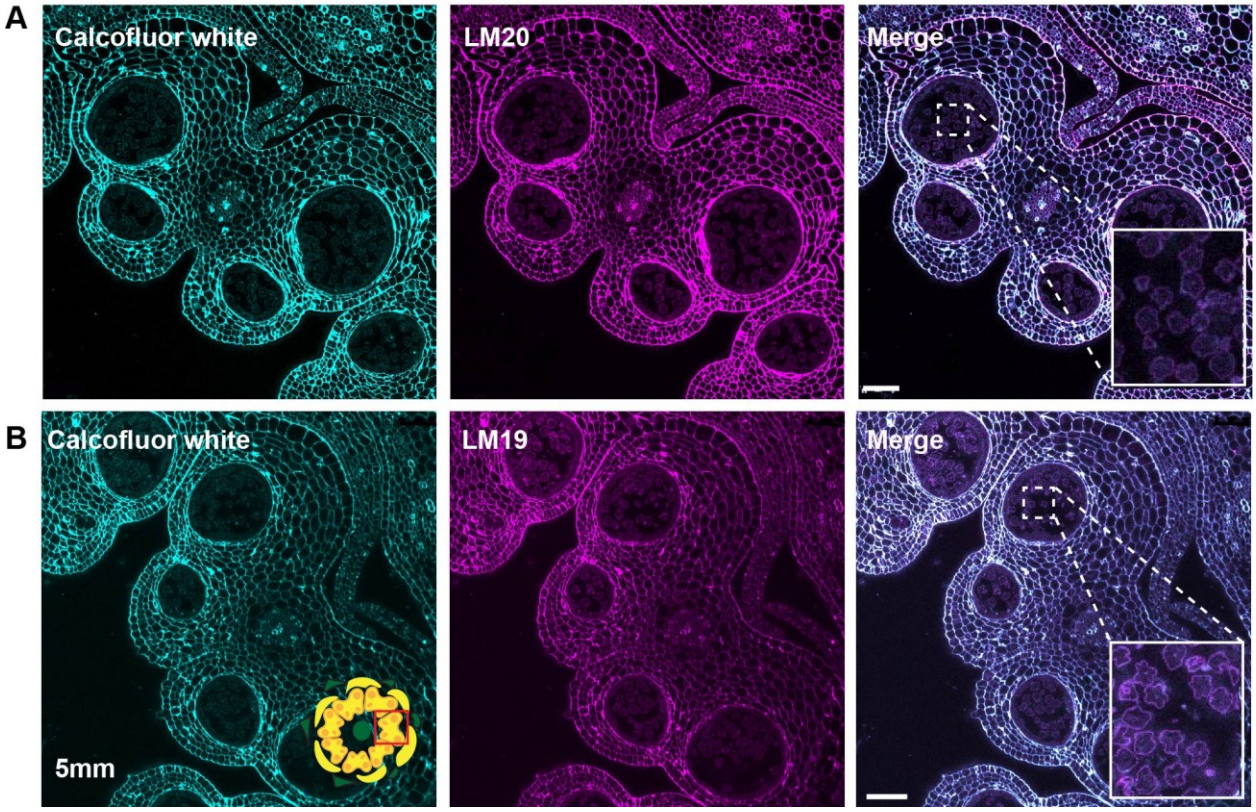

Figure 7 LM20 and LM19 immunostaining of the 5mm bud anthers.

Fluorescent micrographs of anther cross sections (500nm) in LR white, of the 5mm bud anther, stained with Calcofluor white and FITC conjugated secondary for LM20 or LM19. Calcofluor white staining (Cyan) (Left). Aniline blue staining (Magenta) (Center). Merged staining (Right). **A.** LM20 staining of the 5mm anther. Right panel inset showing zoomed in view of the microspore wall with the merged staining. **B.** LM19 staining of the 5mm anther. Right panel inset showing zoomed in view of the microspore with the merged staining. Scale bars 50µm.

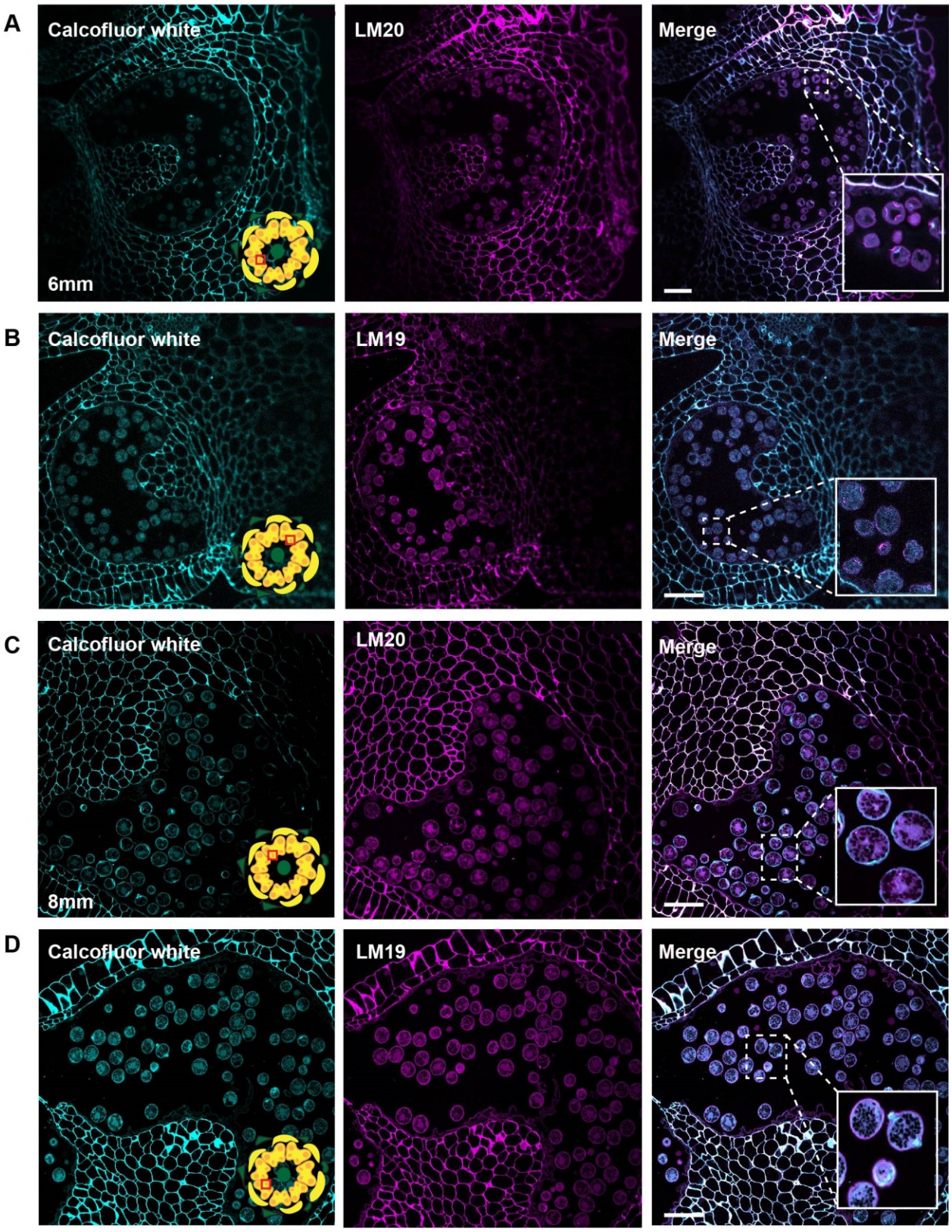
A
Calcofluor white
LM20
Merge
6mm
B
Calcofluor white
LM19
Merge
C
Calcofluor white
LM20
Merge
8mm
D
Calcofluor white
LM19
Merge

Figure 8 LM20 and LM19 immunostaining of the 6mm and 8mm bud anthers.

Fluorescent micrographs of anther cross sections (500nm) in LR white, of the 6mm and 8mm bud anther, stained with Calcofluor white and FITC conjugated anti-rat secondary for LM20 or LM19. Calcofluor white staining (Cyan) (Left). Aniline blue staining (Magenta) (Center). Merged staining (Right). **A.** LM20 staining of the 6mm anther. Right panel inset showing zoomed in view of the pollen wall with the merged staining. **B.** LM19 staining of the 6mm anther. Right panel inset showing zoomed in view of the pollen with the merged staining. **C.** LM20 staining of the 8mm anther. Right panel inset showing zoomed in view of the pollen wall with the merged staining. **D.** LM19 staining of the 8mm anther. Right panel inset showing zoomed in view of the pollen wall with the merged staining. Scale bars 50μm.

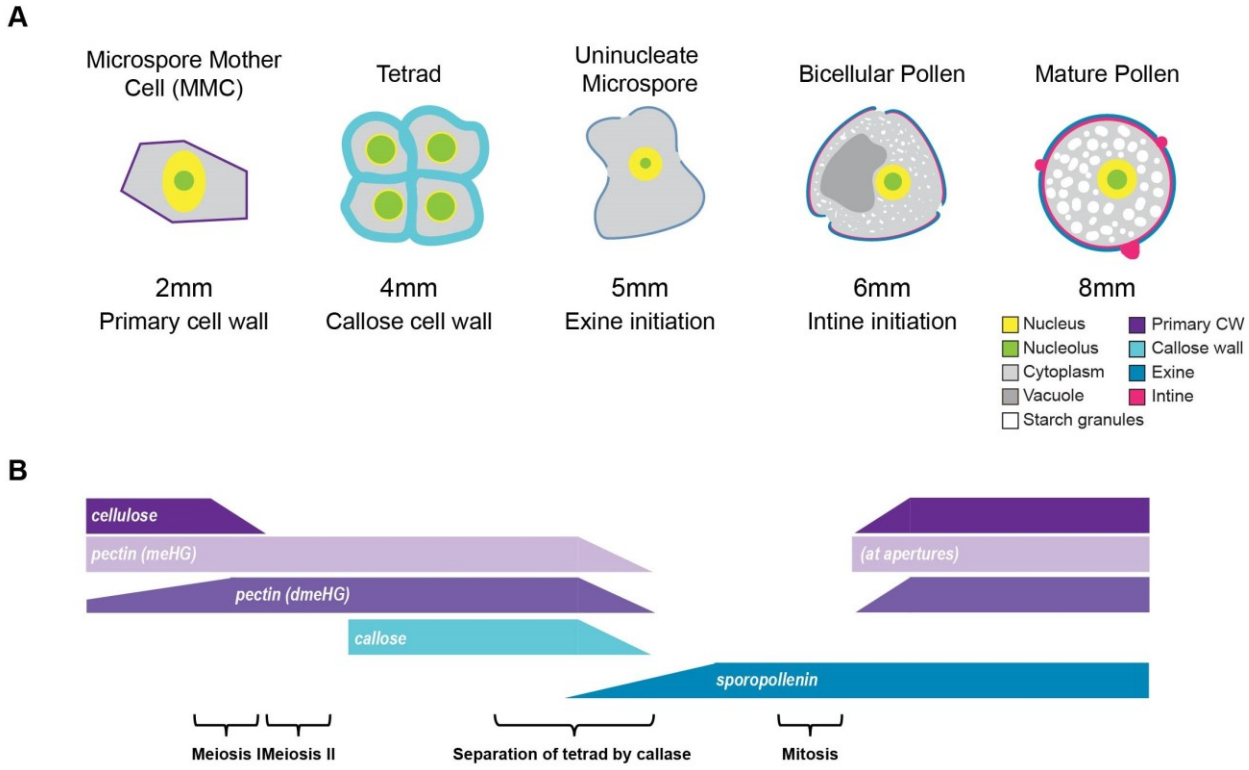

Figure 9 Summary of tomato pollen wall development process.

A. Graphic summary of the major hallmarks of tomato pollen development timeline. The pollen development stage is given above and the bud length corresponding to each stage is given below, along with the major cell wall identities. **B.** Cell wall polymer changes during development. The cellulose of the primary cell wall of the MMC breaks down at the 2mm bud stage. Following meiosis, the tetrad cells are surrounded by a thick callose and pectin wall which is broken down to separate the tetrad cells into free uninucleate microspores. Exine deposition by the tapetal cells begins at the 5mm bud stage and continues through pollen maturation. The deposition of the cellulose and pectin which make up the intine initiates at the 6mm bud stage and also continues through maturation. meHG deposition at the bicellular pollen stage is initially limited to the aperture regions, later spreading to the whole intine.

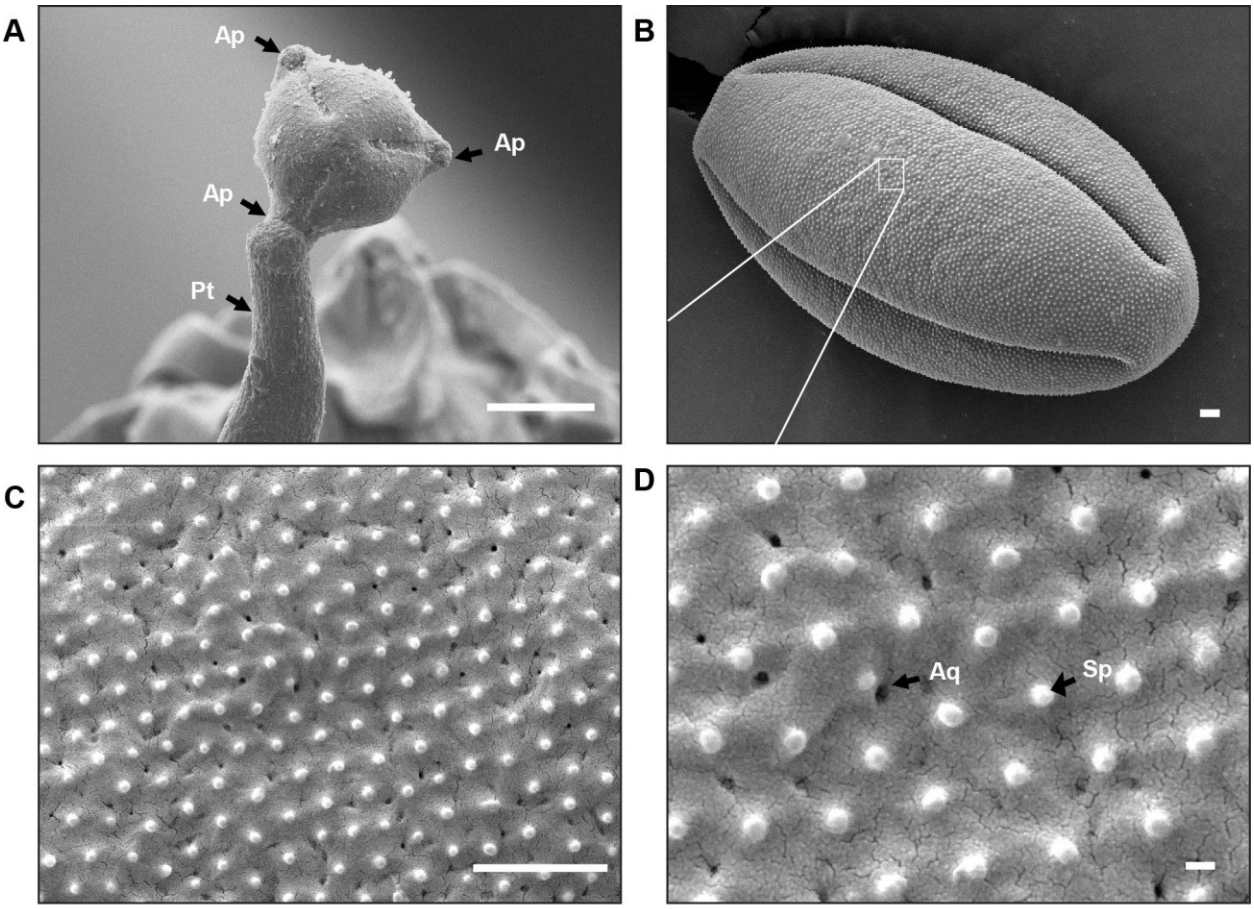

Supplemental Figure 1 Structure of tomato pollen grain surface.

A. Scanning electron micrograph (SEM) of tomato pollen growing a pollen tube. Arrows mark the apertures (Ap) and pollen tube (Pt). **B.** SEM of a mature pollen grain. **C.** Close-up of the box insert from **B.** showing exine patterning. **D.** SEM of pollen wall. Arrow marks the Sp, exine spines and Aq, aquapores. Scale bars 10μm (**A**, top left), 1μm (**B**, top right), 1μm (**C**, bottom left), 100nm (**D**, bottom right).

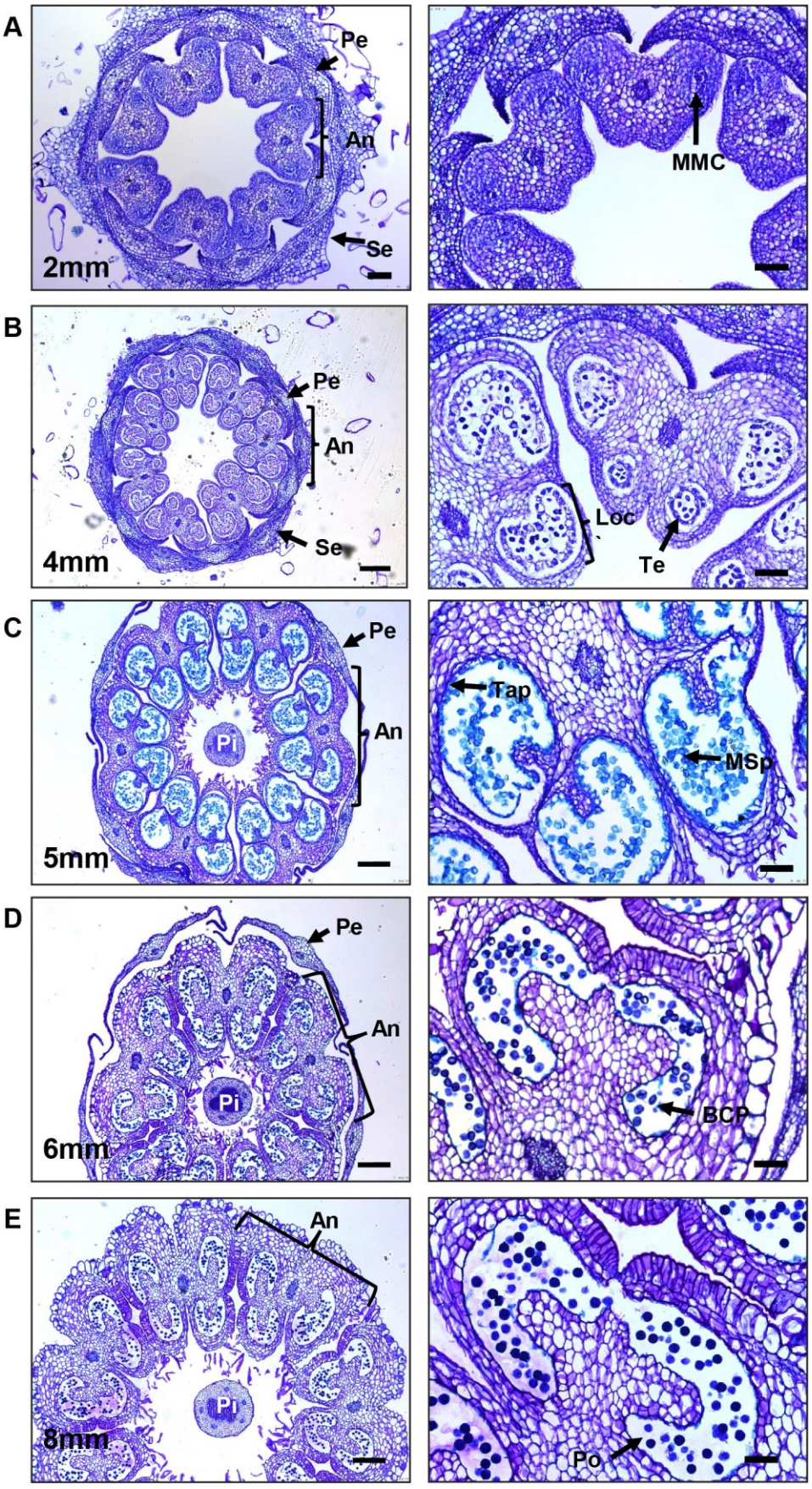
A
Pe
An
Se
2mm
MMC
B
Pe
An
Se
4mm
Loc
Te
C
Pe
An
Pi
5mm
Tap
MSp
D
Pe
An
Pi
6mm
BCP
E
An
Pi
8mm
Po

Supplemental Figure 2 Structure of tomato anther during pollen development.

Micrographs of paraffin embedded anther sections stained with toluidine blue. **A.** Sections of 2mm bud. Arrows mark the apertures (Ap) and pollen tube (Pt). **B.** Sections of 4mm bud. **C.** Sections of 5mm bud. **D.** Sections of 6mm bud. **E.** Sections of 8mm bud. Arrow marks the Pe, petal; An, anther; Se, sepal; Pi, pistil; MMC, microspore mother cell; Loc, locule; Te, tetrad; Tap, tapetum; MS, microspore; BCP, bicellular pollen; Scale bars **A.** 75μm (Left) 50μm (Right) **B. C. D. E.** 200 75μm (Left) 50μm.

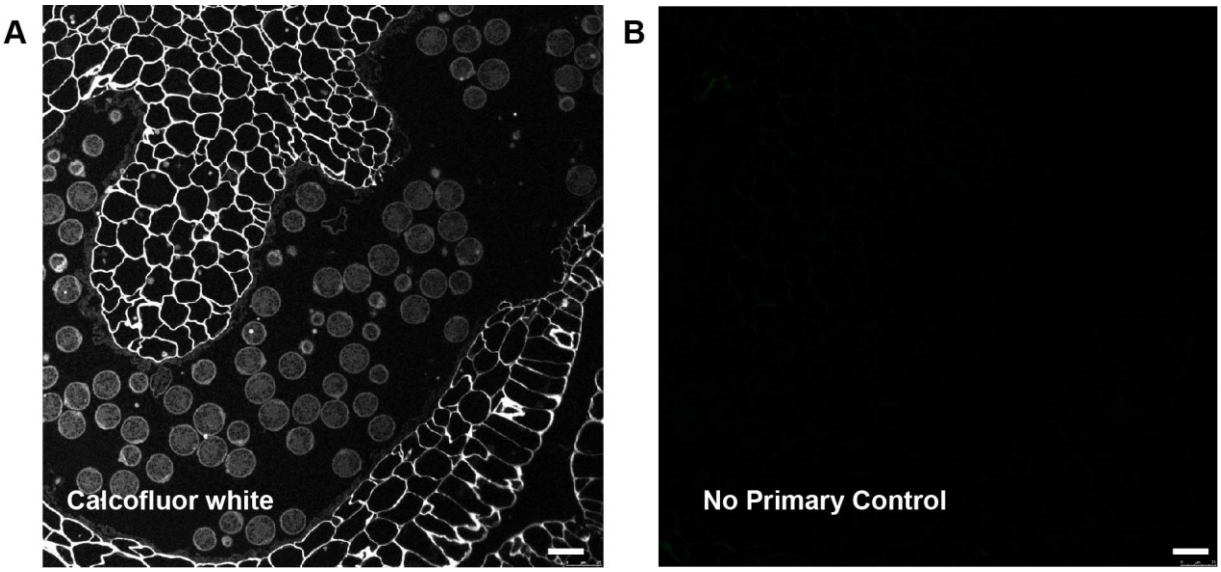

Supplemental Figure 3 No primary antibody control for LM antibody staining.

Fluorescent micrographs of anther cross sections (500nm) in LR white, of 8mm bud anther, stained with Calcofluor white and FITC conjugated secondary antibody only. **A.** Calcofluor white staining (Left). **B.** FITC conjugated secondary only. Scale bars 25μm.

References

Aarts, M. G. ., Hodge, R., Kalantidis, K., Florack, D., Wilson, Z. A., Mulligan, B. J., Stiekema, W. J., Scott, R., & Pereira, A. (1997). The Arabidopsis MALE STERILITY 2 protein shares similarity with reductases in elongation/condensation complexes. *The Plant Journal* 12, 615-623. https://doi.org/10.1046/j.1365-313X.1997.00615.x

Banks, H. (2003). Structure of pollen apertures in the detarieae sensu stricto (Leguminosae: Caesalpinioideae), with particular reference to underlying structures (Zwischenkörper). *Annals of Botany*, *92*(3), 425–435. https://doi.org/10.1093/aob/mcg155

Bashir, M. E. H., Lui, J. H., Palnivelu, R., Naclerio, R. M., & Preuss, D. (2013). Pollen lipidomics: lipid profiling exposes a notable diversity in 22 allergenic pollen and potential biomarkers of the allergic immune response. *PLoS ONE*, *8*(2) e57566. https://doi.org/10.1371/journal.pone.0057566

Blackmore, S., Wortley, A. H., Skvarla, J. J., & Rowley, J. R. (2007). Pollen wall development in flowering plants. *New Phytologist* 174(3), 483-498.

Bosch, M., & Hepler, P. K. (2005). Pectin methylesterases and pectin dynamics in pollen tubes. *The Plant Cell*, *17*(12), 3219–3226. https://doi.org/10.1105/tpc.105.037473

Brukhin, V., Hernould, M., Gonzalez, N., & Chevalier, C. (2003). Flower development schedule in tomato Lycopersicon esculentum cv. sweet cherry. *Sexual Plant Reproduction*, *15*, 311–320. https://doi.org/10.1007/s00497-003-0167-7

Canales, C., Bhatt, A. M., Scott, R., & Dickinson, H. (2002). EXS, a putative LRR receptor kinase, regulates male germline cell number and tapetal identity and promotes seed development in Arabidopsis. *Current Biology*, *12*(02), 1718–1727.

Cankar, K., Kortstee, A., Toonen, M. A. J., Wolters-Arts, M., Houbein, R., Mariani, C., Ulvskov, P., Jorgensen, B., Schols, H. A., Visser, R. G. F., & Trindade, L. M. (2014). Pectic arabinan side chains are essential for pollen cell wall integrity during pollen development. *Plant Biotechnology Journal*, *12*(4), 492–502. https://doi.org/10.1111/pbi.12156

Cannon, M. C., Terneus, K., Hall, Q., Tan, L., Wang, Y., Wegenhart, B. L., Chen, L., Lamport, D. T. A. A., Chen, Y., & Kieliszewski, M. J. (2008). Self-assembly of the plant cell wall requires an extensin scaffold. *Proceedings of the National Academy of Sciences of the United States of America*, *105*(6), 2226–2231. https://doi.org/10.1073/pnas.0711980105

Carvalho, R. F., Campos, M. L., Pino, L. E., Crestana, S. L., Zsögön, A., Lima, J. E., Benedito, V. A., & Peres, L. E. P. (2011). Convergence of developmental mutants into a single tomato model system: “Micro-Tom” as an effective toolkit for plant development research. *Plant Methods*, *7*(1), 1–14. https://doi.org/10.1186/1746-4811-7-18

Chasan, R. (1992). Breaching the callose wall. *The Plant Cell*, *4*, 745–749.

Chebli, Y., Kaneda, M., Zerzour, R., & Geitmann, A. (2012). The cell wall of the Arabidopsis pollen tube-spatial distribution, recycling, and network formation of polysaccharides. *Plant Physiology*, *160*(4), 1940–1955. https://doi.org/10.1104/pp.112.199729

Choi, H., Jin, J., Choi, S., Hwang, J., Kim, Y., Suh, M. C., & Lee, Y. (2011). An ABCG / WBC-type ABC transporter is essential for transport of sporopollenin precursors for exine formation in developing pollen. *The Plant Journal*, 65:181–193. https://doi.org/10.1111/j.1365-313X.2010.04412.x

Christiaens, S., Van Buggenhout, S., Ngouémazong, E. D., Vandevenne, E., Fraeye, I., Duvetter, T., Van Loey, A. M., & Hendrickx, M. E. (2011). Anti-homogalacturonan antibodies: A way to explore the effect of processing on pectin in fruits and vegetables? *Food Research International*, *44*(1), 225–234. https://doi.org/10.1016/j.foodres.2010.10.031

Dobritsa, A. A., Geanconteri, A., Shrestha, J., Carlson, A., Kooyers, N., Coerper, D., Urbanczyk-wochniak, E., Bench, B. J., Sumner, L. W., Swanson, R., & Preuss, D. (2011). A large-scale genetic screen in Arabidopsis to identify genes involved in pollen exine production. *Plant Physiology*, *157*(2), 947–970. https://doi.org/10.1104/pp.111.179523

Dobritsa, A. A., & Reeder, S. H. (2017). Formation of pollen apertures in Arabidopsis requires an interplay between male meiosis, development of INP1-decorated plasma membrane domains, and the callose wall. *Plant Signaling and Behavior*, *12*(12), 1–4. https://doi.org/10.1080/15592324.2017.1393136

Dong, X., Hong, Z., Sivaramakrishnan, M., Mahfouz, M., & Verma, D. P. S. (2005). Callose synthase (CalS5) is required for exine formation during microgametogenesis and for pollen viability in Arabidopsis. *The Plant Journal*, 42: 315–328. https://doi.org/10.1111/j.1365-313X.2005.02379.x

Edlund, A. F., Swanson, R., & Preuss, D. (2004). Pollen and stigma structure and function: The role of diversity in pollination. *Plant Cell*, *16*: S84–S97. https://doi.org/10.1105/tpc.015800

Edlund, A. F., Zheng, Q., Lowe, N., Kuseryk, S., Ainsworth, K. L., Lyles, R. H., Sibener, S. J., & Preuss, D. (2016). Pollen from Arabidopsis thaliana and other Brassicaceae are functionally omniaperturate. *American Journal of Botany*, *103*(6), 1006–1019. https://doi.org/10.3732/ajb.1600031

El-Ghazaly, G., & Jensen, W. A. (1986). Studies of the development of wheat (Triticum aestivum) pollen:I. Formation of the pollen wall and ubisch bodies. *Grana*, *25*(1), 1–29. https://doi.org/10.1080/00173138609429929

Fang, K., Wang, Y., Yu, T., Zhang, L., Baluška, F., Šamaj, J., & Lin, J. (2008). Isolation of de-exined pollen and cytological studies of the pollen intines of *Pinus bungeana* Zucc. Ex Endl. and *Picea wilsonii* Mast. *Flora: Morphology, Distribution, Functional Ecology of Plants*, *203*(4), 332–340. https://doi.org/10.1016/j.flora.2007.04.007

Flores-Tornero, M., Anoman, A. D., & Ros, R. (2015). Lack of phosphoserine phosphatase activity alters pollen and tapetum development in *Arabidopsis thaliana*. *Plant Science*, *235*, 81–88. https://doi.org/10.1016/j.plantsci.2015.03.001

Francis, K. E., Lam, S. Y., & Copenhaver, G. P. (2006). Separation of Arabidopsis Pollen Tetrads Is Regulated by *QUARTET1* , a Pectin Methylesterase Gene. *Plant Phisiology*, *142*, 1004–1013. https://doi.org/10.1104/pp.106.085274

Furness, C. A. (2007). Why does some pollen lack apertures? A review of inaperturate pollen in eudicots. *Botanical Journal of the Linnean Society*, *155*(1), 29–48. https://doi.org/10.1111/j.1095-8339.2007.00694.x

Furness, C. A., & Rudall, P. J. (2004). Pollen aperture evolution - A crucial factor for eudicot success? *Trends in Plant Science*, *9*(3), 154–158. https://doi.org/10.1016/j.tplants.2004.01.001

Giorno, F., Wolters-Arts, M., Grillo, S., Scharf, K. D., Vriezen, W. H., & Mariani, C. (2010). Developmental and heat stress-regulated expression of HsfA2 and small heat shock proteins in tomato anthers. *Journal of Experimental Botany*, *61*(2), 453–462. https://doi.org/10.1093/jxb/erp316

Giorno, F., Wolters-Arts, M., Mariani, C., & Rieu, I. (2013). Ensuring reproduction at high temperatures: The heat stress response during anther and pollen development. *Plants*, *2*(3), 489–506. https://doi.org/10.3390/plants2030489

Gómez, J. F., Talle, B., & Wilson, Z. A. (2015). Anther and pollen development: A conserved

developmental pathway. *Journal of Integrative Plant Biology*, *57*(11), 876–891. https://doi.org/10.1111/jipb.12425

Herburger, K., & Holzinger, A. (2016). Aniline blue and calcofluor white staining of callose and cellulose in the streptophyte green algae Zygnema and Klebsormidium. *Bio-Protocol*, *6*(20), 6–10. https://doi.org/10.21769/bioprotoc.1969

Heslop-Harrison, J. (1968). Pollen Wall Development. *Science*, *161*(3838), 230–237. https://doi.org/10.1126/science.161.3838.230

Hess, M. W., & Frosch, A. (1994). Subunits of forming pollen exine and Ubisch bodies as seen in freeze substituted *Ledebouria socialis* Roth (Hyacinthaceae). *Protoplasma*, *182*(1–2), 10–14. https://doi.org/10.1007/BF01403683

Hess, Michael W. (1993). Cell-wall development in freeze-fixed pollen: Intine formation of *Ledebouria socialis* (Hyacinthaceae). *Planta*, *189*(1), 139–149. https://doi.org/10.1007/BF00201354

Hsiao, A., Yeung, E. C., Ye, Z., & Chye, M. (2015). The Arabidopsis Cytosolic Acyl-CoA-Binding proteins play combinatory roles in pollen development. *Plant and Cell Physiology*, *56*, 322–333. https://doi.org/10.1093/pcp/pcu163

Ishiguro, S., Nishimori, Y., Yamada, M., Saito, H., Suzuki, T., Nakagawa, T., Miyake, H., Okada, K., & Nakamura, K. (2010). The Arabidopsis *FLAKY POLLEN1* gene encodes a 3-hydroxy-3-methylglutaryl- coenzyme a synthase required for development of tapetum-specific organelles and fertility of pollen grains. *Plant and Cell Physiology*, *51*(6), 896–911. https://doi.org/10.1093/pcp/pcq068

Jacobowitz, J. R., Doyle, W. C., & Weng, J. (2019). PRX9 and PRX40 Are extensin peroxidases essential for maintaining tapetum and microspore cell wall integrity during arabidopsis anther development. *The Plant Cell*, *31*, 848–861. https://doi.org/10.1105/tpc.18.00907

Jiang, J., Zhang, Z., & Cao, J. (2013). Pollen wall development: The associated enzymes and metabolic pathways. *Plant Biology*, *15*(2), 249–263. https://doi.org/10.1111/j.1438-8677.2012.00706.x

Kravchik, M., Stav, R., Belausov, E., & Arazi, T. (2019). Functional characterization of microRNA171 family in Tomato. *Plants*, *8*(1). https://doi.org/10.3390/plants8010010

Lee, J. T. Y., & Chow, K. L. (2012). SEM sample preparation for cells on 3D scaffolds by freeze-drying and HMDS. *Scanning*, *34*(1), 12–25. https://doi.org/10.1002/sca.20271

Leroux, C., Bouton, S., Fabrice, T. N., Mareck, A., Guénin, S., Fournet, F., Ringli, C., Pelloux, J., Driouich, A., Lerouge, P., Lehner, A., & Mollet, J. (2015). PECTIN METHYLESTERASE48 is involved in Arabidopsis pollen grain germination. *Plant Physiology*, *167*, 367–380. https://doi.org/10.1104/pp.114.250928

Li, W. L., Liu, Y., & Douglas, C. J. (2017). Role of glycosyltransferases in pollen wall primexine formation and exine patterning. *Plant Physiology*, *173*(1), 167–182. https://doi.org/10.1104/pp.16.00471

Luis da Costa, M., Lopes, A. L., Amorim, M. I., & Coimbra, S. (2017). Immunolocalization of AGPs and pectins in *Quercus suber* gamethophytic structures. *Plant Germline Development: Methods and*

Protocols, Methods in Molecular Biology, 1669, 117-137*September*. https://doi.org/10.1007/978-1-4939-7286-9

Lyu, M., Yu, Y., Jiang, J., Song, L., Liang, Y., Ma, Z., Xiong, X., & Cao, J. (2015). *BcMF26a* and *BcMF26b* are duplicated polygalacturonase genes with divergent expression patterns and functions in pollen development and pollen tube formation in *Brassica campestris*. *PLOS ONE*, 10(7), e0131173. https://doi.org/10.1371/journal.pone.0131173

Ma, X., Wu, Y., & Zhang, G. (2021). Formation pattern and regulatory mechanisms of pollen wall in Arabidopsis. *Journal of Plant Physiology*, *260*, *153388*. https://doi.org/10.1016/j.jplph.2021.153388

Matamoro-Vidal, A., Raquin, C., Brisset, F., Colas, H., Izac, B., Albert, B., & Gouyon, P. H. (2016). Links between morphology and function of the pollen wall: An experimental approach. *Botanical Journal of the Linnean Society*, *180*(4), 478–490. https://doi.org/10.1111/boj.12378

Mollet, J. C., Leroux, C., Dardelle, F., & Lehner, A. (2013). Cell wall composition, biosynthesis and remodeling during pollen tube growth. *Plants (Basel)*, 2(1), 107–147. https://doi.org/10.3390/plants2010107

Müller, F., Xu, J., Kristensen, L., Wolters-Arts, M., De Groot, P. F. M., Jansma, S. Y., Mariani, C., Park, S., & Rieu, I. (2016). High-temperature-induced defects in tomato (*Solanum lycopersicum*) anther and pollen development are associated with reduced expression of B-class floral patterning genes. *PLOS ONE*, *11*(12), e0167614. https://doi.org/10.1371/journal.pone.0167614

Ogawa, M., Kay, P., Wilson, S., & Swain, S. M. (2009). ARABIDOPSIS DEHISCENCE ZONE POLYGALACTURONASE1 required for cell separation during reproductive development in Arabidopsis. *The Plant Cell*, *21*, 216–233. https://doi.org/10.1105/tpc.108.063768

Owen, H. A., & Makaroff, C. A. (1995). Ultrastructure of microsporogenesis and microgametogenesis in *Arabidopsis thaliana* (L.) Heynh. ecotype Wassilewskija (Brassicaceae). *Protoplasma*, *185*(1–2), 7–21. https://doi.org/10.1007/BF01272749

Paxson-sowders, D. M., Dodrill, C. H., Owen, H. A., & Makaroff, C. A. (2001). DEX1, a novel plant protein , is required for exine pattern formation during pollen development in Arabidopsis. *Plant Physiology*, *127*, 1739–1749. https://doi.org/10.1104/pp.010517.is

Paxson-Sowders, D. M., Owen, H. A., & Makarow', C. A. (1997). A comparative ultrastructural analysis of exine pattern development in wild-type Arabidopsis and a mutant defective in pattern formation. *Protoplasma*, *198*, 53–65. https://link.springer.com/content/pdf/10.1007%2FBF01282131.pdf

Persson, S., Paredez, A., Carroll, A., Palsdottir, H., Doblin, M., Poindexter, P., Khitrov, N., Auer, M., & Somerville, C. R. (2007). Genetic evidence for three unique components in primary cell-wall cellulose synthase complexes in Arabidopsis. *Proceedings of the National Academy of Sciences of the United States of America*, *104*(39), 15566–15571. https://doi.org/10.1073/pnas.0706592104

Petersen, B. L., Macalister, C. A., Petersen, B. L., & Ulvskov, P. (2021). Plant protein O-arabinosylation. *Frontiers in Plant Science*, *12*(March). https://doi.org/10.3389/fpls.2021.645219

Phan, H. A., Iacuone, S., Li, S. F., & Parish, R. W. (2011). The MYB80 transcription factor is required for

pollen development and the regulation of tapetal programmed cell death in *Arabidopsis thaliana*. *The Plant Cell*, *23*(6), 2209–2224. https://doi.org/10.1105/tpc.110.082651

Picken, A. J. F. (1984). A review of pollination and fruit set in the tomato (*Lycopersicon esculentum Mill.*). *Journal of Horticultural Science*, *59*(1), 1–13. https://doi.org/10.1080/00221589.1984.11515163

Piffanelli, P., & Murphy, D. J. (1998). Novel organelles and targeting mechanisms in the anther tapetum. *Trends in Plant Science*, *3*(7), 250–252. https://doi.org/10.1016/S1360-1385(98)01260-6

Piffanelli, P., Ross, J. H. E., & Murphy, D. J. (1998). Biogenesis and function of the lipidic structures of pollen grains. *Sexual Plant Reproduction*, 65–80.

Polowick, P L; Sawhney, V, K. (1993a). An ultrastructural study of pollen development in tomato (*Lycopersicon esculentum*). I. Tetrad to early binucleate microspore stage. *Canadian Journal of Botany*, 71(8):1039-1047.

Polowick, P L; Sawhney, V, K. (1993b). Differentiation of the tapetum during microsporogenesis in tomato (*Lycopersicon esculentum Mill* .), with special reference to the tapetal cell wall. *Annals of Botany*, *72*(6), 595–605.

Polowick, P. L., & Sawhney, V. K. (1992). Ultrastructural changes in the cell wall, nucleus and cytoplasm of pollen mother cells during meiotic prophase I in *Lycopersicon esculentum* (Mill.). *Protoplasma*, 169, 139–147.

Pressman, E., Peet, M. M., & Pharr, D. M. (2002). The effect of heat stress on tomato pollen characteristics is associated with changes in carbohydrate concentration in the developing anthers. *Annals of Botany*, *90*(5), 631–636. https://doi.org/10.1093/aob/mcf240

Preuss, D., Lemieux, B., Yen, G., & Davis, R. W. (1993). A conditional sterile mutation eliminates surface components from Arabidopsis pollen and disrupts cell signaling during fertilization. *Genes and Development*, *7*(6), 974–985. https://doi.org/10.1101/gad.7.6.974

Quilichini, T. D., Douglas, C. J., & Samuels, A. L. (2014). New views of tapetum ultrastructure and pollen exine development in *Arabidopsis thaliana*. *Annals of Botany*, 114(6):1189-201. https://doi.org/10.1093/aob/mcu042

Quilichini, T. D., Friedmann, M. C., Samuels, A. L., & Douglas, C. J. (2010). ATP-Binding Cassette Transporter G26 is required for male fertility and pollen exine formation in Arabidopsis. *Plant Physiology*, *154*, 678–690. https://doi.org/10.1104/pp.110.161968

Rejón, J. D., Delalande, F., Schaeffer-Reiss, C., Alché, J. de D., Rodríguez-García, M. I., Van Dorsselaer, A., & Castro, A. J. (2016). The pollen coat proteome: At the cutting edge of plant reproduction. *Proteomes*, *4*(1), 1–23. https://doi.org/10.3390/proteomes4010005

Renzaglia, K. S., Lopez, R. A., Welsh, R. D., Owen, H. A., & Merced, A. (2020). Callose in sporogenesis: novel composition of the inner spore wall in hornworts. *Plant Systematics and Evolution*, *306*(2), 1–9. https://doi.org/10.1007/s00606-020-01631-5

Rhee, S. Y., Osborne, E., Poindexter, P. D., & Somerville, C. R. (2003). Microspore separation in the

quartet3 mutants of Arabidopsis is impaired by a defect in a developmentally regulated polygalacturonase required for pollen mother cell wall degradation. *Plant Physiology*, *133*(3), 1170–1180. https://doi.org/10.1104/pp.103.028266

Schnabelrauch, L. S., Kieliszewski, M. J., Upham, B. L., Alizedeh, H., & Lamport, D. T. A. (1996). Isolation of pl4.6 extensin peroxidase from tomato cell suspension cultures and identification of Val-Tyr-Lys as putative intramolecular cross-link site. *The Plant Journal*, ;9(4):477-89.

Scott, R. J., Spielman, M., & Dickinson, H. G. (2004). Stamen Structure and Function. *The Plant Cell*, *16*, 46–61. https://doi.org/10.1105/tpc.017012.sequentially

Shi, Jianxin, Cui, M., Yang, L., Kim, Y. J., & Zhang, D. (2015). Genetic and biochemical mechanisms of pollen wall development. *Trends in Plant Science*, *20*(11), 741–753. https://doi.org/10.1016/j.tplants.2015.07.010

Shi, Jing, Tan, H., Yu, X., Liu, Y., Liang, W., Ranathunge, K., Franke, R. B., Schreiber, L., Wang, Y., Kai, G., Shanklin, J., & Zhang, D. (2011). Defective pollen wall is required for anther and microspore development in rice and encodes a fatty acyl carrier protein reductase. *The Plant Cell*, *23*, 2225–2246. https://doi.org/10.1105/tpc.111.087528

Shi, X., Sun, X., Zhang, Z., Feng, D., Zhang, Q., Han, L., Wu, J., & Lu, T. (2015). GLUCAN SYNTHASE-LIKE 5 (GSL5) plays an essential role in male fertility by regulating callose metabolism during microsporogenesis in rice. *Plant and Cell Physiology*, *5*, 497–509. https://doi.org/10.1093/pcp/pcu193

Souza, C. D. A., Kim, S. S., Koch, S., Kienow, L., Schneider, K., Mckim, S. M., Haughn, G. W., Kombrink, E., & Douglas, C. J. (2009). A novel Fatty Acyl-CoA synthetase is required for pollen development and sporopollenin biosynthesis in Arabidopsis. *The Plant Cell*, *21*, 507–525. https://doi.org/10.1105/tpc.108.062513

Sridharan, G., & Shankar, A. A. (2012). Toluidine blue : A review of its chemistry and clinical utility. *Journal of Oral and Maxillofacial Pathology*, *16*(2), 251–255. https://doi.org/10.4103/0973-029X.99081

Suárez-Cervera, M., Arcalís, E., Le Thomas, A., & Seoane-Camba, J. A. (2002). Pectin distribution pattern in the apertural intine of *Euphorbia peplus L. (Euphorbiaceae)* pollen. *Sexual Plant Reproduction*, *14*(5), 291–298. https://doi.org/10.1007/s00497-001-0121-5

Suzuki, T., Narciso, J. O., Zeng, W., van de Meene, A., Yasutomi, M., Takemura, S., Lampugnani, E. R., Doblin, M. S., Bacic, A., & Ishiguro, S. (2017). Kns4/upex1: A type II arabinogalactan β-(1,3)-galactosyltransferase required for pollen exine development. *Plant Physiology*, *173*(1), 183–205. https://doi.org/10.1104/pp.16.01385

Takebe, N., Nakamura, A., Watanabe, T., Miyashita, A., Satoh, S., & Iwai, H. (2020). Cell wall Glycine-rich Protein2 is involved in tapetal differentiation and pollen maturation. *Journal of Plant Research*, *133*(6), 883–895. https://doi.org/10.1007/s10265-020-01223-x

Taylor, L. P., & Hepler, P. K. (1997). Pollen germination and tube growth. *Annual Reveiw Plant*

Physiology and Plant Molecular Biology, *48*, 461–491. https://doi.org/10.1007/978-3-642-02301-9_13

Verhertbruggen, Y., Marcus, S. E., Haeger, A., Ordaz-ortiz, J. J., & Knox, J. P. (2009). An extended set of monoclonal antibodies to pectic homogalacturonan. *Carbohydrate Research*, *344*(14), 1858–1862. https://doi.org/10.1016/j.carres.2008.11.010

Verlag, F., Wakabayashi, K., Hoson, T., & Huber, D. J. (2003). Methyl de-esterification as a major factor regulating the extent of pectin depolymerization during fruit ripening: a comparison of the action of avocado (*Persea americana*) and tomato (*Lycopersicon esculentum*) polygalacturonases. *Journal of Plant Physiology*, *673*, 667–673.

Wan, L., Zha, W., Cheng, X., Liu, C., Lv, L., Liu, C., Wang, Z., Du, B., Chen, R., Zhu, L., & He, G. (2011). A rice beta-1,3-glucanase gene Osg1 is required for callose degradation in pollen development. *Planta*, 309–323. https://doi.org/10.1007/s00425-010-1301-z

Wang, R., & Dobritsa, A. A. (2018). Exine and Aperture patterns on the pollen surface: their formation and roles in plant reproduction. *Annual Plant Reviews,* 1, 1–40. https://doi.org/10.1002/9781119312994.apr0625

Yu, J., Meng, Z., Liang, W., Behera, S., Kudla, J., Tucker, M. R., Luo, Z., Chen, M., Xu, D., Zhao, G., Wang, J., Zhang, S., Kim, Y., & Zhang, D. (2016). A Rice Ca 2+ Binding protein is required for tapetum function and pollen formation. *Plant Physiology*, *172*, 1772–1786. https://doi.org/10.1104/pp.16.01261

Zhang, D., Chen, W., Yu, X., Zhang, K., Shi, J., Oliveira, S. De, Schreiber, L., Shanklin, J., & Zhang, D. (2011). *Male Sterile2* encodes a plastid-localized Fatty Acyl Carrier Protein Reductase required for pollen exine development in Arabidopsis. *Plant Phisiology*, *157*, 842–853. https://doi.org/10.1104/pp.111.181693

Zhang, X., Zhao, G., Tan, Q., Yuan, H., Betts, N., Zhu, L., Zhang, D., & Liang, W. (2020). Rice pollen aperture formation is regulated by the interplay between OsINP1 and OsDAF1. *Nature Plants*, *6*(4), 394–403. https://doi.org/10.1038/s41477-020-0630-6

Zinkl, G. M., Zwiebel, B. I., Grier, D. G., & Preuss, D. (1999). Pollen-stigma adhesion in Arabidopsis : a species-specific interaction mediated by lipophilic molecules in the pollen exine. *Development*, *5440*, 5431–5440.